TITLE

Visualizing subcellular structures in neurons with expansion microscopy

AUTHORS

Logan A. Campbell[1*], Katy E. Pannoni[1*], Niesha A. Savory[2], Dinesh Lal[3], Shannon Farris[1-4#]

AFFILIATIONS

[1]Center for Neurobiology Research, Fralin Biomedical Research Institute, Virginia Tech Carilion, Roanoke, VA, 24016, USA.
[2]School of Neuroscience, Virginia Tech, Blacksburg, VA, 24016, USA.
[3]Virginia Tech Carilion School of Medicine, Roanoke, VA, 24016, USA.
[4]Department of Biomedical Sciences & Pathobiology, Virginia-Maryland College of Veterinary Medicine, Virginia Tech, Blacksburg, VA, 24061, USA.

[*]Authors contributed equally
[#]Lead Contact Farrissl@vtc.vt.edu

Abstract Word Count 174
Introduction, Results, Discussion Word Count 3,573
Figures 6
Tables 3

ABSTRACT

Protein expansion microscopy (proExM) is a powerful technique that crosslinks proteins to a swellable hydrogel to physically expand and optically clear biological samples. The resulting increased resolution (~70 nm) and physical separation of labeled proteins make it an attractive tool for studying the localization of subcellular organelles in densely packed tissues, such as the brain. However, the digestion and expansion process greatly reduces fluorescence signals making it necessary to optimize ExM conditions per sample for specific end goals. Here we describe a proExM workflow optimized for resolving subcellular organelles (mitochondria and the Golgi apparatus) and reporter-labeled spines in fixed mouse brain tissue. By directly comparing proExM staining and digestion protocols, we found that immunostaining before proExM and using a Proteinase K based digestion for 8 hours consistently resulted in the best fluorescence signal to resolve subcellular organelles while maintaining sufficient reporter labeling to visualize spines and trace individual neurons. With these methods, we more accurately quantified mitochondria size and number and better visualized Golgi ultrastructure in reconstructed CA2 neurons of the hippocampus.

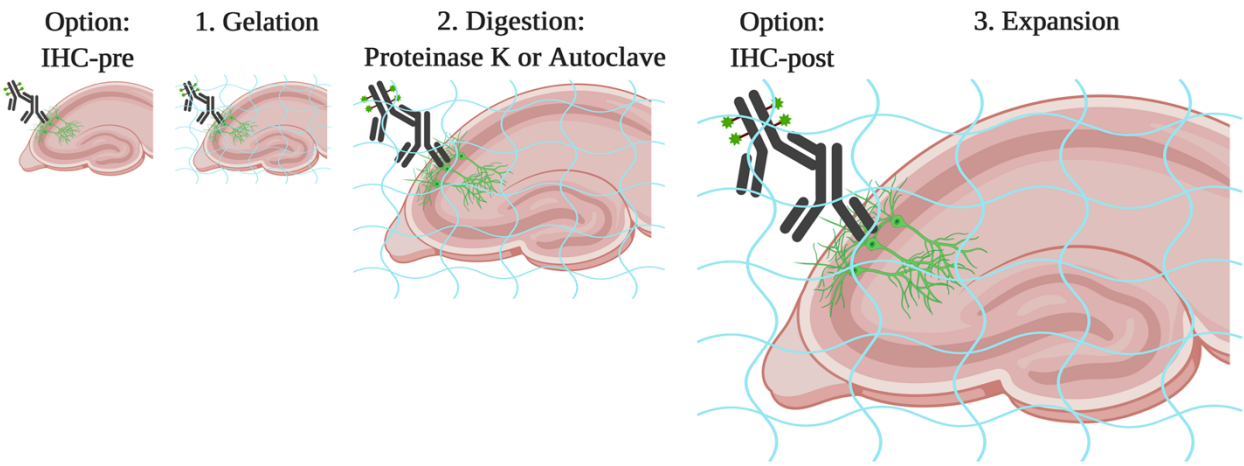

Figure 1: ExM workflow for visualizing subcellular organelles in fixed brain tissue.
Schematic of immunostaining and proExM workflows tested to optimize visualization of organelles in genetically-labeled neurons.

INTRODUCTION

Protein retention expansion microscopy (proExM) is a powerful tool that crosslinks proteins to a swellable hydrogel to optically clear and physically expand tissues up to ~4-fold in volume[1,2]. Because expansion physically separates crosslinked moieties, this technology is particularly useful for visualizing subcellular structures in densely packed tissues, such as the brain. However, one consequence of tissue expansion is a decrease in the fluorescence intensity of labeled proteins primarily due to the digestion process and the dilution of fluorescence signal per unit volume. Various ExM protocols have described different methods for improving fluorescence retention, primarily by modifying fixation, crosslinking, and/or digestion conditions to preserve protein epitopes[2–8]. One common ExM protocol uses a strong protease-based digestion (Proteinase K[2]), but other gentler proteases have also been used (LysC[2,3]), as well as a combination of heat and detergents in place of proteases (e.g. autoclave in an alkaline buffer[2–5]).

Immunostaining can also be done before or after ExM to boost fluorescence[2,3] (Fig. 1), although results are often dependent on the protein epitope and the quality of antibody staining. To improve antibody staining in brain tissue, antigen retrieval is often performed prior to immunostaining via boiling tissue in water or heating tissue in a citrate buffer (pH 6) to expose protein epitopes and reduce nonspecific staining. Here we set out to compare ExM immunostaining and digestion conditions for fluorescently labeled subcellular organelles in perfused brain sections using antibodies that either require or do not require antigen retrieval (COX4-labeling of mitochondria and GOLGA5-labeling of Golgi, respectively). Visualizing the spatial organization of organelles within compartmentalized cells, such as neurons, is important for understanding their function, thus we paid particular attention to conditions that maintained fluorescence signal from genetically-encoded reporters (i.e. enhanced green fluorescent protein, EGFP, and tdTomato). We found that performing IHC, with or without antigen retrieval, prior to

ExM with Proteinase K digestion for 8 hours best preserves fluorescence signal for co-visualizing subcellular organelles and neuronal morphology, including spines. Further, we report our optimized conditions for antibodies against widely used reporters and conclude with protocol considerations for achieving specific end goals.

RESULTS

Proteinase K digestion time impacts fluorescence intensity and expansion factor

Sufficient digestion or homogenization (also referred to as hydrolysis in some protocols) is required to prevent sample distortion during expansion and is highly dependent on digestion conditions, including time, temperature, pH, buffer composition and enzyme quality[1,3,9]. Varying digestion time impacts fluorescence intensity[1] and how much the tissue expands in water, or the expansion factor[5]. To determine the effect of digestion time on the fluorescence intensity of the Amigo2-EGFP reporter line, which predominantly labels hippocampal area CA2 neurons, we performed a time course of enzymatic digestion with Proteinase K as described in the proExM protocol[3]. Initially, we performed the time course on 40-micron vibratome cut sections from perfused adult Amigo2-EGFP mouse brains. Hydrogels were digested for 2, 4, 8 or 16 hours at room temperature. Unfortunately, there was insufficient EGFP signal remaining at the 8 and 16 hour timepoints to directly compare hydrogels across conditions (data not shown). We then repeated the experiment on sections immunostained for GFP prior to ExM and imaged the resulting gels with identical acquisition parameters to directly compare fluorescence intensities and expansion factors (Fig. 2). Importantly, we measured micro expansion factors, or the degree to which cell soma areas expanded versus the commonly reported macro expansion factors calculated by measuring how much the hydrogel expands. We found that average fluorescence intensities diminished as the length of digestion time increased (one-way ANOVA; F-stat: 20.96, p-value: 8.17E-14. N = two animals, 1-2 sections per animal per time point; 159 total cells, 32 ± 4 cells per time point, Fig. 2AB). Further, we found that average expansion factors increased as length of digestion time increased (one-way ANOVA; F-stat: 21.07, p-value: 4.26E-11, Fig. 2CD), resulting in an inverse relationship between fluorescence intensity and expansion factor (Fig. 2E). Interestingly, we did not detect significant decreases in fluorescence intensities from pairwise comparisons between the 8-hr digestion and the 2- or 4-hr digestions (p=0.90 and 0.55, respectively, Tukey's post hoc test, Fig. 2D), despite significant increases in expansion factors between the same comparisons (p=0.001 for each). These data indicate that 8-hr digestion retains the most fluorescence for a sizable expansion factor (~3) that is not significantly different from the overnight expansion factor (p=0.18). However, we note that the fluorescence intensities reported here are corrected for background, and shorter digestion times have greater fluorescence background signal compared with longer digestion times (see Table 1). Regardless of digestion time, we were able to successfully acquire robust fluorescent images at each time point, including overnight (Fig. 2F), as long as immunolabeling was performed prior to ExM.

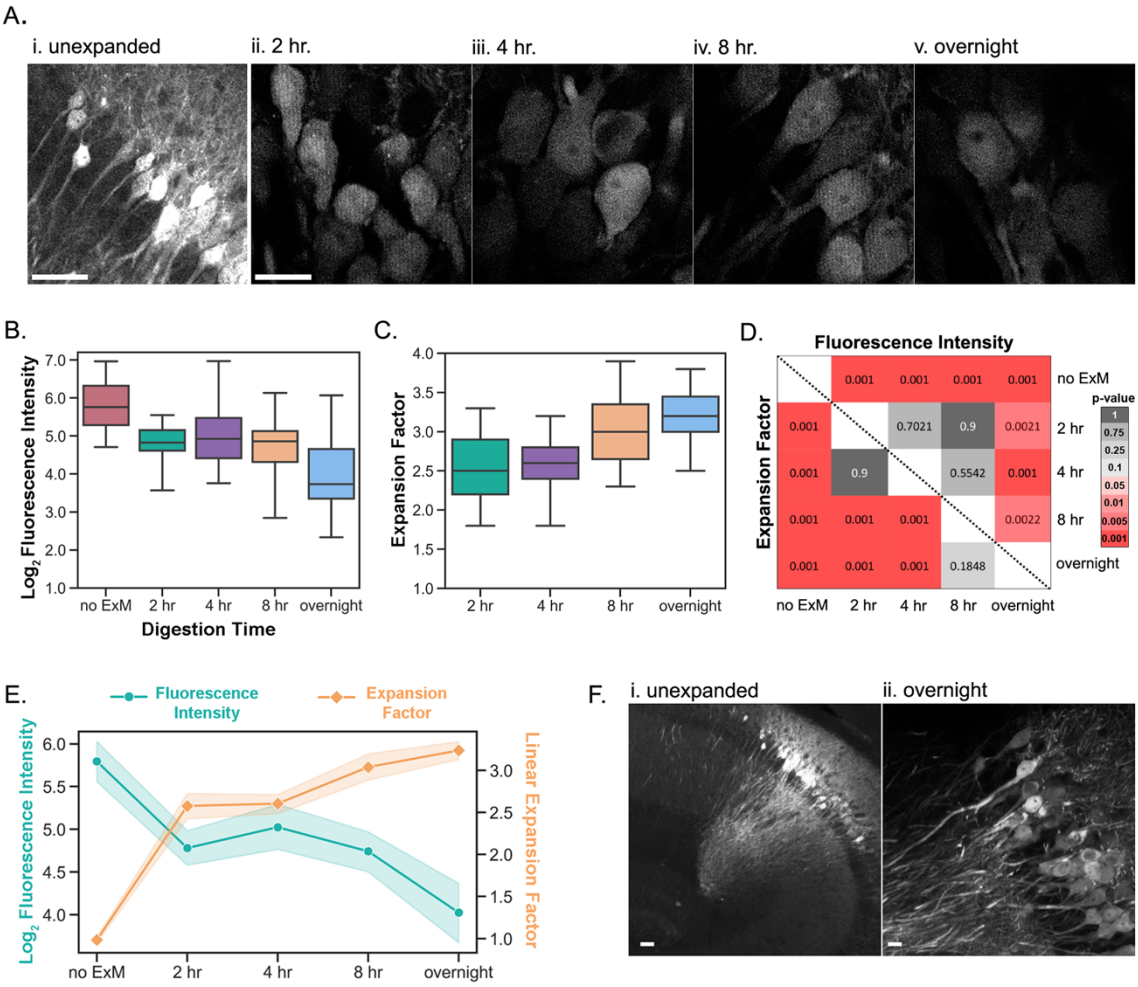

Figure 2: The effect of Proteinase K digestion time on fluorescence intensity and expansion factor.
A) Representative single z-section images of unexpanded (i) and expanded GFP+ CA2 neurons after 2-hour (ii), 4-hour (iii), 8-hour (iv), or overnight (v) digestion with Proteinase K. Image acquisition parameters were identical for each condition, except for the unexpanded condition.
B) GFP fluorescence intensity measured in the cell soma after the different digestion times. Fluorescence was corrected for background and $\log_2$ transformed. Line represents the median. Digestion time had a significant effect on GFP fluorescence (one-way ANOVA; F-stat: 20.96, p-value: 8.17E-14, 32 ± 4 cells per time point from two animals, 159 total cells).
C) Expansion factor of the expanded cell somas in B. Expansion factors were calculated using cell soma areas relative to the average unexpanded cell soma area. Digestion time had a significant effect on expansion factor (one-way ANOVA; F-stat: 21.07, p-value: 4.26E-11).
D) Matrix of p-values visualizing the results of pairwise Tukey's post hoc tests comparing mean fluorescence (upper diagonal) or expansion factor (lower diagonal) at each digestion time point. Matrix is color coded by p-value (red = significant; grey = not significant; α=0.05).
E) Effect of digestion time on fluorescence intensity (cyan; left axis) and expansion factor (orange; right axis). Plot shows the mean and 95% confidence intervals from **B** and **C**.
F) Unexpanded (i) and overnight expanded (ii) max-projection 10X confocal images of GFP+ CA2 cells. Images are the same as in **A**(i) and (v). Imaging parameters were optimized separately to obtain the best image of both. Scale bars = (**A**, **F**) 50 µm.

Cells expand equivalently, independent of section depth

Next we considered if the time-dependent effect of Proteinase K on expansion factor and fluorescence intensity is impacted by tissue depth. We reasoned that cells near the surface may

have greater access to Proteinase K and/or fluorescently-labeled antibodies compared with cells deeper within tissue that may impact expansion factor and/or fluorescence intensity, respectively. To test this, we compared cell soma areas binned by Z-section depth (adjusted by hydrogel thickness) across digestion time points.

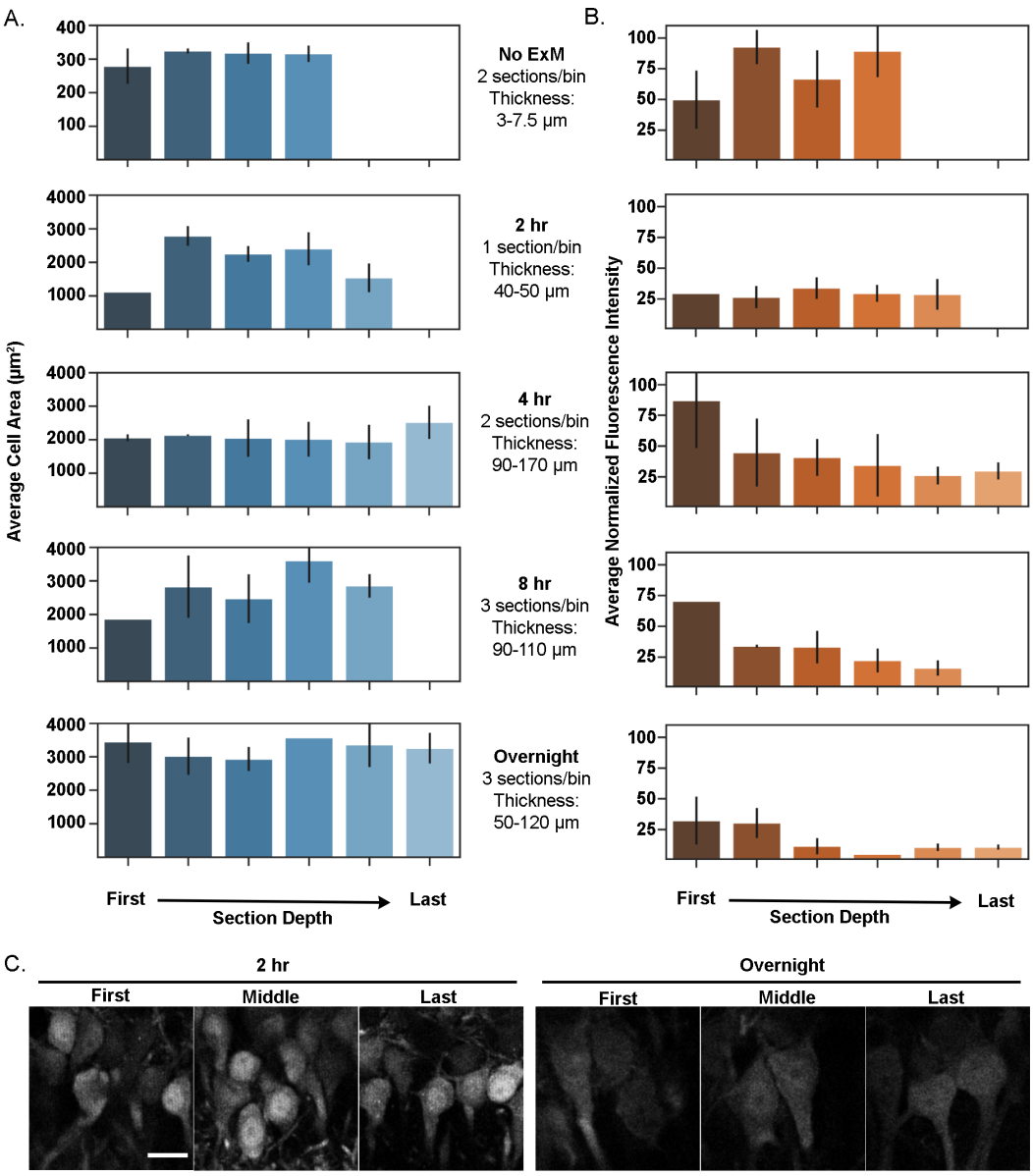

Figure 3: No appreciable effect of tissue depth on expansion factor.
A) Average cell soma area (in μm²) by Z section depth for unexpanded control and digestion conditions. Cell soma area was measured in the Z section with the widest soma diameter. Because of the overall increase in depth with expansion, cells were binned by Z section to achieve ~6 bins per time point. N = 32 ± 4 cells per time point.
B) Background subtracted average cell soma fluorescence by Z section depth. Binning of the data is the same as in A. The data are not $\log_2$ transformed as in Fig 2.
C) Representative confocal images of GFP+ CA2 cell somas after 2-hour (left panel) or overnight (right panel) digestion at three Z-section depths. Cell soma size and fluorescence is variable in the Z dimension in unexpanded conditions, which does not appreciably change under difference digestion conditions. Error bars show the standard deviation. Scale bar is 50μm.

113 We did not detect a systematic difference in cell soma area across z-section depth (Fig. 3),
114 indicating that Proteinase K equivalently digests 40-micron thick tissue, at least by the 2-hr time
115 point. For some time points (e.g. 4- and 8-hrs) fluorescence intensity appeared brighter near the
116 surface compared with deeper sections (Fig. 3B). However, we note this is likely due to optical
117 limits, as fluorescence intensity was not brighter at the far-end surface that has equivalent access
118 to Proteinase K and antibody solutions. We saw similar results with 100-micron thick tissue
119 (data not shown).
120
121 *Immunolabeled organelles are best resolved with IHC prior to ExM*
122 Protease digestion can decrease fluorescence intensity by impacting fluorescently-labeled
123 antibodies and/or target antigen availability. Thus, immunohistochemistry (IHC) labeling before
124 or after ExM (further referred to as IHC-pre and IHC-post, respectively) can be affected, but it is
125 unknown if they equally affect the fluorescence intensity of antibodies that require antigen
126 retrieval. Protease-free digestion protocols (e.g. detergent plus heat created in an autoclave liquid
127 cycle) have been shown to effectively digest hydrogels, and avoids protease-dependent depletion
128 of fluorescence intensity[3]. However, these protocols have not been tested with antibodies that
129 require antigen retrieval. In Figure 4, we directly compared COX4-mitochondria labeling after
130 protease (Proteinase K) or autoclave (i.e. mild digestion) digestion ExM protocols[3]. We further
131 compared these digestion protocols with IHC performed pre (Fig. 4AB) or post ExM (Fig. 4CD).
132 Our optimized protocol for COX4 immunostaining on unexpanded sections (Fig. 4E) requires
133 antigen retrieval (boiling) prior to IHC, thus an antigen retrieval step was included for sections
134 bound for Proteinase K digestion.
135
136 We detected COX4-labeled mitochondria using both Proteinase K and autoclave digestion
137 ExM protocols (Fig. 4), however Proteinase K digested gels performed better with IHC-pre, and
138 autoclave digested gels performed better with IHC-post. Compared with unexpanded COX4-
139 labeled mitochondria, expanded COX4-labeled mitochondria were on average slightly greater in
140 number per cell (ExM: 117.5 ± 5.6, No ExM: 95.8 ± 4.4) and smaller in size (mitochondria size:
141 ExM 0.001 ± 0.0, No ExM 0.003 ± 0.0) after normalizing to cell soma area (total mitochondria
142 area: ExM 422.5 ± 93.7, No ExM 123.8 ± 2.4) (Fig. 4G). To account for potential anisotropic
143 expansion of cell somas, we compared the ratio of nuclear area (measured via DAPI) to the cell
144 soma area (measured via reporter labeling) and found them to be similar on average with and
145 without ExM (ratio: ExM 0.357 ± 0.00, No ExM 0.347 ± 0.01; nuclear area: ExM 1,383.1 ±
146 93.5, No ExM 154.5 ± 7.8; soma area: ExM 3,869.5 ± 259.2, No ExM 443.3 ± 11.8), indicating
147 that the decrease in percent cytoplasmic area of mitochondria (Fig. 4I) is due to better
148 individually resolved expanded mitochondria.
149
150 In regards to reporter labeling, RFP fluorescence only fared well when IHC was done prior to
151 ExM, regardless of digestion method. Thus, for epitopes that require antigen retrieval and/or
152 reporter labeling, IHC-pre-ExM is the preferred method of choice. Note that antigen retrieval

diminishes reporter labeling (RFP and GFP) and explains the difference in RFP intensity between autoclave (Fig. 4Aii) and Proteinase K (Fig. 4Bii) digested gels. If only mitochondria labeling is required, the autoclave digestion protocol performs well with IHC-post. The inferior staining of COX4 with IHC-pre with autoclave digestion compared with IHC-pre with Proteinase K digestion may be due to a lack of antigen retrieval in the former that is achieved by autoclave digestion.

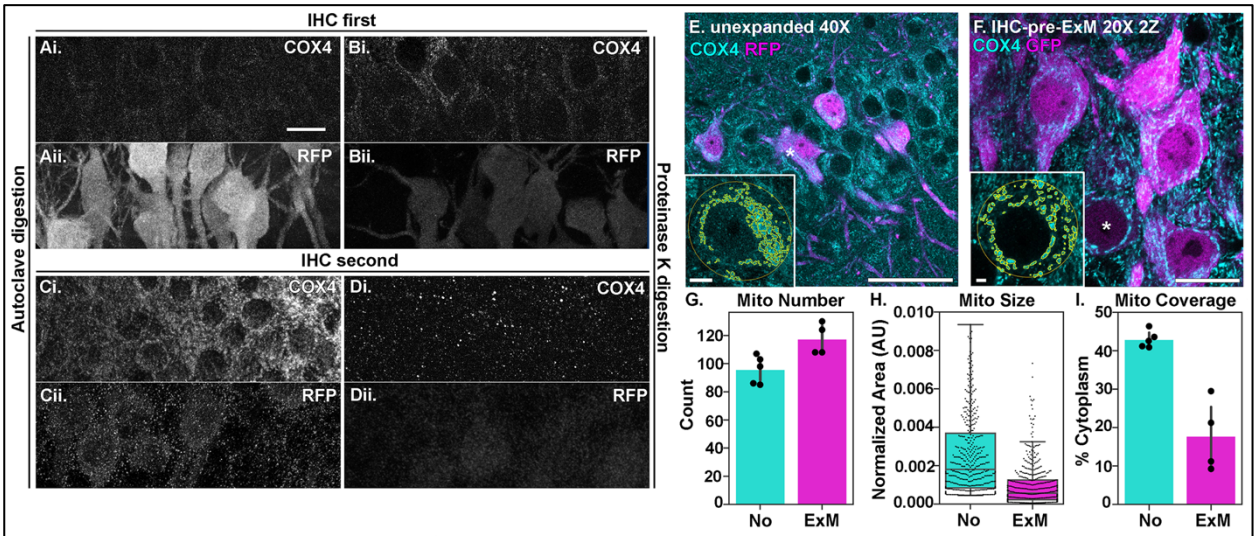

Figure 4: ProExM pipeline comparison for visualizing mitochondria.
A) 20X Max-projection image of a section immunostained for COX4 (i) and RFP (ii) pre-ExM with autoclave digestion. Images in panels A-D were acquired with identical imaging parameters to directly compare conditions. Brightness and contrast were adjusted to the same extent across the entire image.
B) 20X Max-projection image of a boiled section immunostained for COX4 (i) and RFP (ii) pre-ExM with overnight Proteinase K digestion.
C) 20X Max-projection image of a section immunostained for COX4 (i) and RFP (ii) post-ExM with autoclave digestion.
D) 20X Max-projection image of a boiled section immunostained for COX4 (i) and RFP (ii) post-ExM with overnight Proteinase K digestion
E) 40X Max-projection image from a subset of Z sections from a boiled, unexpanded section immunostained for COX4 and RFP. Inset is a single Z section from the indicated representative cell (white asterisk) with mitochondria outlined as quantified in **G-I**. Imaging parameters were optimized per condition in **E-F**.
F) 20X Max-projection image from a subset of Z sections from a boiled section immunostained for COX4 and GFP pre-ExM with overnight Proteinase K digestion as in **B**.
G) The average number of mitochondria per cell in unexpanded **(E)** and expanded **(F)** sections.
H) Mitochondria area per cell (normalized by soma area). Line reflects median and whiskers are twice the inner quartile range.
I) The average percent cytoplasm area (soma area - nuclear area) containing mitochondria. Note that ExM better resolves densely packed mitochondria, resulting in greater number, smaller sized, and fewer percent area per cell soma compared with non-ExM.
Scale bars: 50 µm (**A**,**E**,**F**) and 5 µm (insets).

We next compared the Proteinase K and autoclave ExM protocols with GOLGA5-immunolabeling of Golgi apparatus (Fig. 5), which does not require antigen retrieval. Consistent with our COX4 results, GOLGA5-labeled Golgi were detected with either Proteinase K or autoclave digested protocols. Golgi in expanded sections were well resolved and revealed complex Golgi structure compared with Golgi in unexpanded sections (Fig. 5F). In contrast to our COX4 results, GOLGA5-labeling fared well in both IHC-pre-ExM digestion conditions, likely due to robust GOLGA5-labeling in unboiled sections. Similar to COX4, GOLGA5-labeling post-ExM with Proteinase K digestion was unsuccessful. IHC-pre with autoclave

digestion was not tested. As with RFP reporter labeling, GFP reporter labeling also fared well with IHC-pre and autoclave digestion, albeit at lower intensities than Proteinase K digestion. Thus, GFP and RFP fluorescence retention are comparable when antibody-labeled prior to ExM and they retain more fluorescence with Proteinase K digestion compared with autoclave digestion. It is important to note that we detect qualitative differences in the ability of different reporter antibodies to detect spines, with and without ExM (see Table 3).

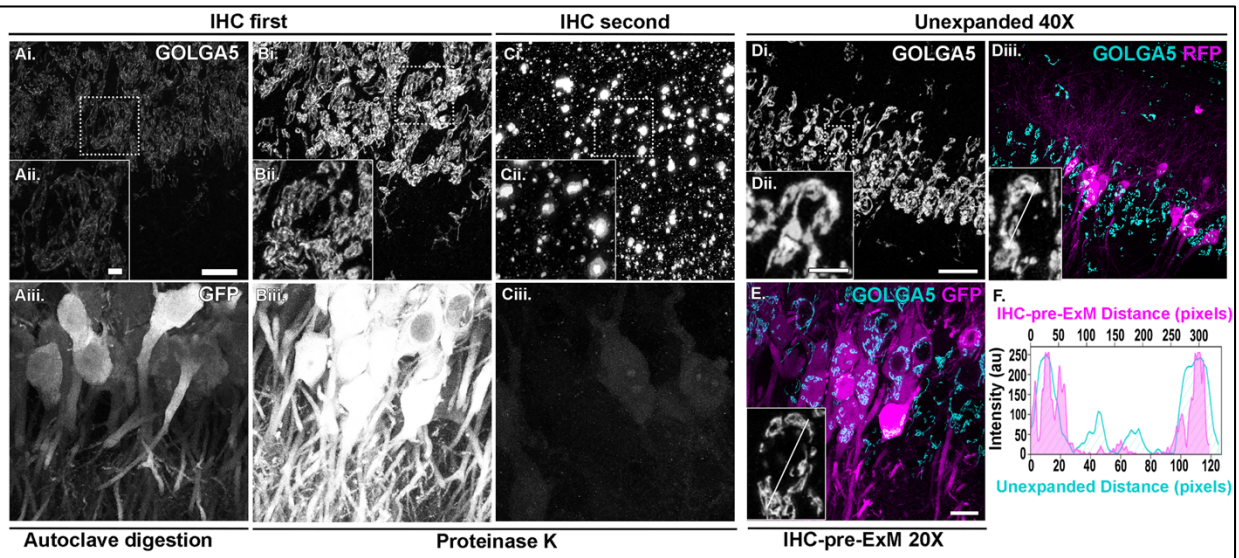

Figure 5: ProExM pipeline comparison for visualizing Golgi.
A) 20X Max-projection image of a section immunostained for GOLGA5 (i) and GFP (iii) pre-ExM with autoclave digestion. (ii) Insets are zoomed images of the dotted box in (i). Images in panels **A**-**C** were acquired with identical imaging parameters to directly compare conditions. Brightness and contrast were adjusted to the same extent across the entire image.
B) 20X Max-projection image of a section immunostained for GOLGA5 (i) and GFP (iii) pre-ExM with overnight Proteinase K digestion.
C) 20X Max-projection image of a section immunostained for GOLGA5 (i) and GFP (iii) post-ExM with overnight Proteinase K digestion.
D) 40X Max-projection of a subset of Z sections from an unexpanded section immunostained for GOLGA5 (i) and RFP (iii). Imaging parameters were optimized per condition in **D**-**E**.
E) 20X Max-projection of a subset of Z sections from image in (**B**) immunostained pre-ExM with overnight Proteinase K digestion. Note the increase in Golgi complexity that is resolved with autoclave or Proteinase K digested gels compared with unexpanded sections, although fluorescence intensity was better retained with Proteinase K digestion.
F) Line plot profile showing the fluorescence intensity of unexpanded Golgi (cyan) and Golgi after IHC-pre-ExM with Proteinase K digestion (magenta). Measured Golgi are insets in **D**iii and **E**.
Scale bars: 50µm (**A**i, **D**i, **E**) and 10µm (**A**ii, **D**ii).

Dendritic spines are best resolved in expanded GFP or RFP-immunolabeled tissue

In addition to resolving subcellular organelles such as mitochondria and Golgi apparatus, the ability to resolve fine dendritic structures such as spines allows us to address questions about function and plasticity at synapses. Thus, we set out to find the optimal combination of ExM conditions for subcellular organelles and reporter antibodies to resolve dendritic spines in our EGFP and tdTomato reporter mice. Table 3 compares spines in unexpanded and expanded tissue, with or without immunolabeling for the reporter protein, and with or without antigen retrieval by boiling or citrate. Expanded samples were immunostained pre-ExM (if at all) and digested overnight with Proteinase K, as described in the methods. To boost the signal of the reporter

187 protein, we tested two antibodies against each EGFP and tdTomato reporters (anti-GFP and anti-
188 RFP, respectively). The ability to resolve dendritic spines in each condition was qualitatively
189 assessed by multiple investigators (not blinded to condition), and indicated by the number of + in
190 the table (from + to ++++). A greater number of + indicates better discrimination of spines and
191 "-" indicates dendritic spines could not be resolved for a given condition. Some conditions in the
192 table have yet to be tested as indicated where applicable.
193

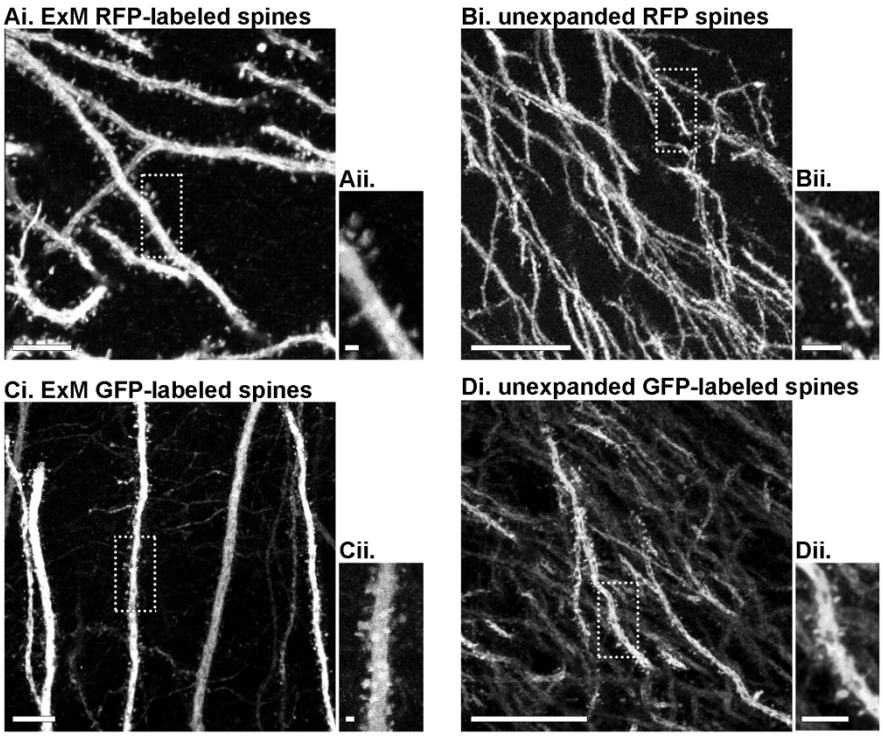

Figure 6: Resolving dendritic spines with ExM.
A) 20X with 3X zoom max-projection image (i) of a section immunostained for RFP pre-ExM with overnight Proteinase K digestion. This mouse received 2 tamoxifen injections. (ii) Insets are 2X zoomed images of the dotted box in (i). All images were acquired with parameters optimal per condition. Brightness and contrast were adjusted per condition across the entire image.
B) 40X with 2X zoom max-projection image of an unexpanded tdTomato section. This mouse received 2 tamoxifen injections.
C) 20X with 2X zoom max-projection image of a section immunostained for GFP pre-ExM with overnight Proteinase K digestion.
D) 40X with 2X zoom max-projection image from an unexpanded section immunostained for GFP. Note the increased background labeling and density of dendritic branches in the unexpanded images, making dendrites more difficult to trace compared with expanded images.
Scale bars: 25μm (**Ai**, **Bi**, **Ci**, **Di**) and 5μm (**Aii**, **Bii**, **Cii**, **Dii**).

194
195
196 Figure 6 shows representative images of dendritic spines for each of the four conditions tested. In
197 general, spines were easier to resolve in tdTomato reporter mice (top panel) than EGFP reporter
198 mice (bottom panel), even with the same ExM and IHC conditions. However, both reporter lines
199 benefited from the addition of IHC to boost the reporter signal. Without an IHC boost, neither
200 reporter line had resolvable spines after ExM (see Table 3), primarily due to a loss of

fluorescence. We saw the best resolution of spines in expanded tdTomato+ tissue that was stained with the rabbit anti-RFP without any antigen retrieval (Fig. 6A; "Am2-icre;tdTomato/RFP-rabbit" in Table 3). We noted that the chicken RFP antibody did not label spines as well as the rabbit RFP antibody ("Am2-icre;tdTomato/RFP-chicken", Table 3), indicating that not all reporter antibodies are equal when it comes to labeling spines. The IHC-pre-ExM condition increased the resolution of tdTomato+ dendritic spines compared with unexpanded and unlabeled tdTomato+ dendritic spines (Fig. 6B). While spines were still visible on tdTomato+ CA2 dendrites without immunostaining or expansion (Fig. 6Bii), we were not able to reliably resolve spines on unexpanded or expanded EGFP+ dendrites without immunostaining ("am2-EGFP", Table 3). With the addition of IHC, however, spines could be resolved on GFP+ dendrites in both expanded (Fig. 6C) and unexpanded tissue (Fig. 6D). Compared to unexpanded tissue with the same IHC conditions, the ExM protocol increases the resolution of spines by increasing their physical size and separation from nearby dendritic branches and reducing background fluorescence (compare Fig. 6C and D) enabling spine morphometric analyses on individually traced neurons.

DISCUSSION

ProExM is a powerful tool that increases the resolution of conventional fluorescence microscopy to ~70 nm and can be performed with tools available in a standard molecular biology laboratory[10,11]. Because a fully expanded hydrogel is mostly water, the optically clear sample is well suited to resolve densely packed organelles and tissues. However, the digestion and expansion process greatly reduces fluorescence retention making it necessary to optimize ExM conditions per sample for specific end goals. Here we described a proExM workflow optimized for resolving subcellular organelles (mitochondria and the Golgi apparatus) and spines in fixed mouse brain tissue. We reliably found that immunostaining before proExM (IHC-pre-ExM) and using a Proteinase K based digestion for 8 hours resulted in the best fluorescence signal to resolve subcellular organelles while maintaining sufficient reporter labeling to visualize spines and trace individual neurons. With these methods, we were able to more accurately quantify mitochondria size and number and better visualize Golgi ultrastructure in reconstructed CA2 neurons of the hippocampus.

Several groups have optimized expansion protocols to visualize subcellular organelles across different sample types, including various cell lines[1,5,8,12–15], rat liver[16], clinical specimens[17], fungi[6,18], songbird[19] and drosophila[20,21]. Others have used ExM to visualize subcellular structures, including mitochondria[1,2,22–24] and/or spines[2,19,22] in brain tissue, but few have systematically analyzed how fluorescence intensities and expansion factors compare across protocols or with unexpanded measurements. This is critically important as several groups have noted discrepancies in micro versus macro expansion factors in other sample types[7,13,16,25–27], including dissimilarities in expansion factors of different subcellular organelles[13] or of subcellular organelles across neighboring cells and tissues[16]. Others, however, have reported minimal to no differences in micro vs macro expansion factors[6,18]. We did not measure macro

242 expansion factors here, but our average micro expansion factors are lower than the commonly
243 reported 4-4.5X macro expansion factor for proExM, which is consistent with other reports using
244 micro expansion factor measurements[13,14] (but see also ref[25]), reinforcing the notion that each
245 sample type needs to be independently optimized and validated for ExM.

246 To determine the optimal digestion time for fluorescence retention in fixed brain sections, we
247 performed a digestion time course and found the greatest drop in fluorescence after the overnight
248 digestion. There was no significant drop in fluorescence between 2, 4 or 8 hours of digestion.
249 However, there was a significant increase in expansion factor during this time period. Expansion
250 factor begins to plateau after 8 hours of digestion, and while there is a slight increase in
251 expansion factor in the overnight condition it is not statistically significant. Therefore, under the
252 conditions used here, a digestion time of 8 hours is ideal for achieving a robust expansion (~3X)
253 without further loss of fluorescence seen with overnight digestion. At all digestion time points,
254 the expansion factor did not systematically vary by depth, indicating that 2 hours in Proteinase K
255 is sufficient for uniform penetration and isotropic expansion in the Z dimension of 40 micron
256 brain sections, as previously reported for thicker sections and longer digestion times[10].

257 In regards to labeling subcellular organelles in fixed brain sections, we were able to visualize
258 expanded mitochondria with a COX4 antibody and expanded Golgi apparatus with a GOLGA5
259 antibody, using either the proteinase K digestion or the mild autoclave digestion. In our hands,
260 the IHC-pre ExM with proteinase K digestion outperformed the other conditions based on
261 fluorescence signal retention for both immunostained organelles and reporter proteins. While
262 EGFP and tdTomato have been reported to have different percent fluorescence retention after
263 ExM[2], they perform comparably when antibody-labeled prior to ExM, as recently reported in
264 cultured cells[28]. They also retain more fluorescence with Proteinase K digestion compared with
265 autoclave digestion. However, if the goal is only to visualize mitochondria, the mild autoclave
266 digestion with IHC-post ExM also produced good COX4 staining, as seen for other mitochondria
267 immunostains, like TOMM20[2]. The GOLGA5 antibody performed decently using IHC-pre ExM
268 and autoclave digestion, which the COX4 antibody did not, likely due to COX4 immunolabeling
269 requiring antigen retrieval. Neither antibody performed well with IHC-post ExM and Proteinase
270 K digestion.

271 Despite diminished fluorescence, ExM afforded better resolution for quantification of
272 subcellular organelles compared to unexpanded organelles. We quantified the number and size of
273 expanded mitochondria and found that the expanded mitochondria were smaller and more
274 numerous than unexpanded mitochondria. This presumably is indicative of tightly packed
275 mitochondria in the unexpanded samples being lumped together that can be separately resolved
276 with expansion. Here, we normalized subcellular measurements (i.e. mitochondria size) to within
277 cell nuclear and cytoplasmic areas. Another study found discrepancies in cell soma vs nuclear
278 expansion factors[16], but here the ratio of nuclear area to cytoplasmic area remained constant

279 between unexpanded and expanded states, indicating isotropic expansion, perhaps due to our
280 longer digestion times.

281 The fine details of the Golgi cisternae were also better resolved after expansion, whereas
282 without expansion the Golgi were smoothened and much of the details lost. For the goal of
283 visualizing reporter-labeled dendritic spines, we found that the addition of IHC-pre ExM was
284 necessary for the resolution of both EGFP+ and tdTomato+ spines. Dendritic spines were best
285 resolved in IHC-pre ExM with Proteinase K digestion with either GFP or RFP antibodies. The
286 ability to label dendritic spines in ExM was antibody dependent, with some antibodies against
287 the same reporter faring better than others under the same IHC conditions.

288 Our lab has begun applying the described proExM methods to answer open questions
289 involving subcellular organelles in neurons. One such open question is whether there is Golgi
290 present in dendrites, or if the Golgi is limited to neuronal cell bodies. It is known that local
291 translation of RNA occurs in dendrites[29]; however, there is conflicting evidence of the existence
292 of Golgi apparatus in the dendrites , which would normally process newly transcribed membrane
293 bound proteins. Using combined GOLGA5-labeling of Golgi apparatus and reporter neuron
294 labeling with the proExM protocol described here, we do not detect GOLGA5 staining outside
295 the cell soma or very proximal dendrites, consistent with reports that canonical Golgi markers
296 are retained in the soma and not present in distal dendrites[24,31,32].
297
298 *Considerations for subcellular imaging of expanded samples*
299 The benefits of expansion come at several costs, including diminished signal concentration,
300 hydrogel mechanical integrity and movement, and increased imaging volume and time[5]. Here we
301 comment on the proposed workarounds[2,3,11] for these issues that have or have not worked well
302 for subcellular imaging of expanded brain sections.
303
304 Expansion microscopy substantially increases the thickness of a sample, which limits its ability
305 to be imaged with standard high magnification microscope objectives with limited working
306 distances. It can be expected that the gel thickness will be equivalent to 4-fold the depth of the
307 gelation chamber. Further, keeping the tissue in plane during gel chamber assembly is difficult,
308 often resulting in increased sample z-distance. Minimizing tissue thickness (40 microns versus
309 100 microns) and using a single coverslip for the gelation chamber helped minimize gel
310 thickness without sacrificing ability to reconstruct neurons.
311
312 Loss of fluorescence due to the digestion of antibodies or epitopes and dilution of fluorescent
313 molecules per unit volume can result in low contrast samples not suitable for high resolution
314 imaging even with overexpressed fluorescent reporter proteins. We found that performing IHC
315 beforehand and limiting the Proteinase K digestion to 8 hours largely negated this issue. When
316 the fluorescence signal is insufficient, imaging in low concentrations of PBS (0.5X PBS instead
317 of 0.0001X PBS or water) substantially improved the contrast by increasing the concentration of

318 fluorescent molecules per area. This will decrease the expansion factor, but in our hands, even a
319 2-3-fold expansion in optically clear tissue produces better resolved images of subcellular
320 structures than unexpanded tissue.
321
322 Hydrogel movement during imaging is a common issue for us. Because gels expand 4-fold in x,
323 y and z compared with unexpanded brain sections, tile scans are required to reconstruct entire
324 neurons even at 10x (see Fig. 2Fii for a 10x single field of view of expanded neurons). Tile
325 scanning increases the length of time required to image a gel and thus worsens gel shift. Gel shift
326 was most noticeable while imaging on an upright microscope equipped with a water immersion
327 lens, since the gel can easily shift when submerged. Gel shift was less noticeable when imaging
328 either on an inverted scope or on an upright scope with air objectives (if the gel was dried for 30
329 minutes to adhere to the glass bottom plate), but these options negatively impact objective
330 working distance or resolution, respectively. To minimize gel shift during upright imaging with a
331 water dipping lens, we applied the following techniques to stabilize the gel in the imaging
332 chamber (50 mm WillCo Well). Following full expansion in water, we surrounded the gel with
333 2% agarose in the imaging chamber. This noticeably reduced gel movement during acquisition of
334 single images but shift was still detected during longer tile scans. We also tested re-embedding
335 the gelated sample in an unexpandable gel and covalently linking it to the glass imaging dish[2].
336 This completely eliminated movement of the gel and allowed us to take long tile scans on an
337 upright or inverted microscope. Unexpectedly, however, this also seemed to dampen the
338 fluorescence signal, which was irreversible.
339
340 **Table 1: Digestion time course.** Table showing mean expansion factor and fluorescence
341 intensities (FI) for each digestion time point and the unexpanded control. Also included is the
342 average background fluorescence intensity ("BG FI"), the normalized $\log_2$ transformed
343 fluorescence, and the number of cells ("N Cells") for each digestion condition.

Digest Time	Exp Factor	Mean FI	BG FI	$\log_2$ Norm FI	N Cells
no ExM	1.0 (±0.02)	69.0 (±5.39)	7.24 (±0.63)	5.795 (±0.12)	31
2 hour	2.6 (±0.08)	32.91 (±1.93)	3.56 (±0.4)	4.78 (±0.10)	29
4 hour	2.6 (±0.06)	42.79 (±4.77)	4.21 (±0.24)	5.024 (±0.14)	33
8 hour	3.0 (±0.08)	32.43 (±2.43)	2.34 (±0.01)	4.742 (±0.13)	35
overnight	3.2 (±0.05)	22.84 (±2.72)	2.28 (±0.03)	4.025 (±0.18)	31

344
345
346 **Table 2: Antibodies and conditions.** Table showing primary and secondary antibody conditions
347 used for expansion microscopy.

Primary Antibody	Host	Clonality	Supplier	Catalogue #	Antigen retrieval	Concentration	Incubation
GFP	Chicken	Polyclonal IgY	Abcam	ab13970	Not Required	1:500	72+ hrs at RT

GFP Booster Atto 488	Alpaca	Monocolonal VHH	Chromotek	gba488-100	Not Required	1:200	72+ hrs at RT
RFP	Rabbit	Polyclonal IgG	Rockland	600-401-379	Not Requred	1:500	72+ hrs at RT
RFP	Chicken	Polyclonal IgY	Rockland	600-901-379	Not Required	1:250	72+hrs at RT
GOLGA5/Golgin-84	Rabbit	Polyclonal IgG	Abcam	ab224040	Not Required	1:500	72+ hrs at RT
COX4	Rabbit	Polyclonal IgG	Synaptic Systems	298 003	5 min at 100C	1:500	72+hrs at RT
ERGIC-53/P58	Rabbit	Polyclonal IgG	Sigma Aldrich	E1031	Citrate at 80C	1:600	72+ hrs at RT
ST3GAL5	Rabbit	Polyclonal IgG	Sigma Aldrich	AV46358	Citrate at 80C	1:250	72+ hrs at RT
Secondary Antibody							
Goat anti Mouse IgG (H+L) Alexa 488	Goat	Polyclonal IgG	Invitrogen	A11029	NA	1:500	48+ hrs at RT
Goat anti Mouse IgG (H+L) Alexa 546	Goat	Polyclonal IgG	Invitrogen	A11030	NA	1:500	48+ hrs at RT
Goat anti Rabbit IgG (H+L) Alexa 488	Goat	Polyclonal IgG	Invitrogen	A11034	NA	1:500	48+ hrs at RT
Goat anti Rabbit IgG (H+L) Alexa 546	Goat	Polyclonal IgG	Invitrogen	A11035	NA	1:500	48+ hrs at RT
Goat anti Chicken IgY (H+L) Alexa 488	Goat	Polyclonal IgY	Invitrogen	A11039	NA	1:500	48+ hrs at RT
Goat anti Chicken IgY (H+L) Alexa 546	Goat	Polyclonal IgY	Invitrogen	A11040	NA	1:500	48+ hrs at RT

Table 3: Detection of reporter labeled spines

Tissue/Antibody	ExM (protK)	IHC (pre-ExM)	Spines
Am2-GFP	unexpanded	no IHC	+
		ag-no IHC	-
	expanded	no IHC	-
		ag-no IHC	-
Am2-GFP/GFP-chicken	unexpanded	IHC	++
		ag-IHC	+
	expanded	IHC	+++
		ag-IHC	++
Am2-GFP/GFP booster-alpaca	unexpanded	IHC	+
		ag-IHC	-
	expanded	IHC	-
		ag-IHC	nt
Am2-icre;tdTomato	unexpanded	no IHC	++

		ag-no IHC	+
	expanded	no IHC	-
		ag-no IHC	nt
Am2-icre;tdTomato/RFP-chicken	unexpanded	IHC	+++
		ag-IHC	+
	expanded	IHC	++
		ag-IHC	+
Am2-icre;tdTomato/RFP-rabbit	unexpanded	IHC	++++
		ag-IHC	nt
	expanded	IHC	++++
		ag-IHC	nt
- not detected; + rare SLM only; ++ OK; +++ Good; ++++ Excellent; nt Not tested			

352 **METHODS**
353
354 **Animals**
355 Adult male and female Amigo2-EGFP (RRID:MMRRC 033018-UCD, bred for at least 10
356 generations onto C57BL/6J background) or Amigo2-icreERT2;RosaTdTomato transgenic mice
357 were used. Amigo2-icreERT2;RosaTdTomato mice were generated by crossing Amigo2-
358 icreERT2 mice[33] to Ai14 mice (Jax #007914). Amigo2-icreER;ROSA-TdTomato mice were
359 given 2 or 3 daily intraperitoneal injections of tamoxifen (Sigma T5648, 100mg/kg freshly
360 dissolved daily in 100% ethanol then diluted 10-fold in corn oil and heated at 60C for 1 hour
361 until in solution). Mice were group-housed under a 12:12 light/dark cycle with access to food
362 and water *ad libitum*. All procedures were approved by the Animal Care and Use Committee of
363 Virginia Tech.
364
365 **Immunofluorescence**
366 Mice were anesthetized with 150mg/kg fatal plus solution and perfused with ice-cold 4%
367 paraformaldehyde. Amigo2-icreERT2;RosaTdTomato mice were perfused one week post
368 tamoxifen injections. Brains were dissected and post-fixed for at least 24 hours before sectioning
369 40 µm thick sections in the horizontal plane on a vibratome (Leica VT1000S). Sections to be
370 stained with COX4 underwent antigen retrieval by boiling free floating sections in 1.7ml tubes
371 for 3 min in nanopure water. All sections were washed in PBS and blocked for at least 1 hour in
372 5% Normal Goat Serum (NGS)/0.3% Triton-100x. See Table 3 for primary and secondary
373 antibodies and conditions. Antibodies were diluted in blocking solution and sections were
374 incubated for 72+ hours at room temperature (RT). After several rinses in PBS-T (0.3% Triton-
375 100x), sections were incubated in secondary antibodies for 48 hours at RT. Prior to imaging,
376 unexpanded sections were washed in PBS-T and mounted under Vectashield fluorescence media
377 with 4′,6-diamidino-2-phenylindole (DAPI) (Vector Laboratories).
378
379 **Protein expansion microscopy solution preparation**
380 Solutions were prepared as described by Asano et. al 2018[3]. Anchoring stock solution was
381 prepared by dissolving Acryloyl-X, SE (ThermoFisher A20770) in DMSO (1:100 w/v) and
382 stored at -20C. Monomer solution components were prepared by dissolving Sodium Acrylate in
383 npH20 (33% w/v, Sigma 408220), Acrylamide in npH20 (50% w/v, Sigma A9099), N, N'-
384 Methylenebisacylamide in npH20 (2% w/v, Sigma M7279). Monomer working solution was
385 prepared by adding 2.25mL of 33% SA solution (8.6% w/v), 0.5 mL of 50% Acrylamide
386 solution (2.5% w/v), 0.75 mL of 2% N,N-Methylenebisacrylamide solution (0.15% w/v), 4 mL
387 of 5M NaCl (11.7% w/v), and 1 mL of 10X PBS. Inhibitor stock was prepared by dissolving 4-
388 Hydroxy-TEMPO (0.5% w/v, Sigma 176141) in npH2O and initiator stock was made by
389 dissolving Ammonium persulfate in npH2O (10% w/v, Sigma 248614). Accelerator solution was
390 prepared by diluting TEMED in npH2O (10% v/v, Sigma T7024) immediately before use. All
391 solutions except the TEMED accelerator were prepared before use and stored at -20C.

392
393 **Protein expansion microscopy**
394 4X protein expansion microscopy (proExM) was carried out on horizontal mouse brain sections
395 containing dorsal hippocampus as described in Asano et al 2018[3]. Sections were incubated
396 overnight in Acryloyl-X stock/PBS (1:100, ThermoFisher, A20770) at RT in the dark. Following
397 incubation, the slices were washed twice with PBS for 15 minutes each at RT. The gelation
398 solution was prepared by adding 384 uL of monomer solution, 8 uL 4-Hydroxy-TEMPO
399 inhibitor (1:200 w/v, Sigma Aldrich, 176141), 8uL TEMED accelerator (10% v/v, Sigma
400 Aldrich, T7024), and lastly 8uL of APS initiator (10% w/v, Sigma Aldrich, 248614) for each
401 section. Sections were then incubated in the gelation solution for 30-45 minutes at 4C in the
402 dark. Gelated sections were placed on gelation chambers constructed from microscope slides
403 with coverslips as spacers. Our gelation chambers produce gels with the thickness of two type
404 No. 1.5 coverslips (~0.3mm thick). The chambers were filled with gelation solution and allowed
405 to incubate at 37 C for 2 hours in a humidified container. Following gelation incubation, the
406 gelation chamber was deconstructed to uncover the gelated brain section. To remove the gel
407 from the chamber, digestion solution without Proteinase K was applied and a coverslip was used
408 to gently remove the sample. Digestion solution containing Proteinase K (8U/mL, New England
409 BioLabs, P8107S) was applied to gels and allowed to digest for 2-16 hours (see Results) at room
410 temperature. Upon completion of digestion, gels were stained with DAPI (Sigma Aldrich,
411 D9542, 1:10,000 in PBS) for 10 minutes at room temperature with shaking. The gels were then
412 washed twice for 10 minutes with npH2O to remove excess DAPI and fully expand the gel.
413
414 *Stabilizing ExM Gels with Agarose*
415 To prevent movement during imaging, gels were fully expanded in water or 0.001X PBS in
416 WillCo wells (HBSB-5040) and reversibly immobilized by applying liquid 2% agarose around
417 and on top of the gel (in areas not containing tissue). Following application, the gel embedded
418 with agarose was placed at 4C for at least 15 minutes to allow the agarose to fully solidify prior
419 to imaging.
420
421 *Re-embedding and Linking Gels to Imaging Dish*
422 Re-embedding and covalently linking gels to a WillCo well allowed long-term imaging without
423 gel shifting as described by Tillberg et al 2016[2]. First, the gel was completely expanded in water
424 and then incubated in a non-expanding re-embedding solution (3% w/v acrylamide, 0.15% w/v
425 N,N-methylenebisacylamide, 0.05% w/v APS, 0.05% w/v TEMED, and 5mM Tris). The gels
426 were incubated with shaking at room temperature for 20 minutes. The gel was then transferred to
427 a Bind-Silane treated WillCo Well plate and covered with a coverslip. Fresh re-embedding
428 solution was then lightly applied surrounding the sample, which was then incubated at 37C for
429 1.5-2hrs without shaking. Once the re-embedding solution gelated, the coverslip was removed
430 from the covalently linked gel and could be imaged.
431

432 *Bind Silane Treatment of Imaging Dishes*
433 Immediately before use, imaging dishes were treated with a bind silane solution as described by
434 Tillberg et al 2016[2]. Before bind silane treatment, imaging dishes were briefly washed with
435 npH2O, 100% Ethanol, and then allowed to dry. Bind silane solution (80% v/v EtOH, 2% v/v
436 acetic acid, 0.05% v/v Bind-Silane) was then applied with shaking for 5 minutes. The dish was
437 then washed with 100% EtOH and allowed to dry before usage.
438
439 *Digestion Time Course Experiment*
440 To assess the effect of digestion time on tissue expansion and fluorescence retention, we ran a
441 digestion time course experiment by varying the amount of time the ExM gels were in digestion
442 solution-- either 2 hours, 4 hours, 8 hours or 16 hours (overnight). The brains of two Amigo2-
443 EGFP mice (One male and one female, 21-23 weeks old) were processed as above. During a
444 pilot run, we noted that samples with digestion > 2 hours lost the majority of EGFP fluorescence,
445 making it impossible to acquire images with identical parameters for direct comparison.
446 Therefore, to boost the EGFP signal, approximately ten sections per brain (two sections per
447 condition per mouse) were first immunostained in a 24-well plate as described in the
448 immunohistochemistry methods, with a primary chicken antibody against EGFP (Abcam,
449 ab13970; 1:500 concentration) at RT for 3 days, followed by a secondary antibody (Invitrogen
450 Alexa-488, A11039; 1:500 concentration) incubation for 48 hours. As a control, a few sections
451 were set aside after immunostaining to mount on slides without expanding.
452
453 Sections processed for ExM were anchored in Acryloyl-X overnight, washed twice with 1X PBS
454 and incubated in gelation solution for 30 min at 4C the following day (see "Protein Expansion
455 Methods" for more detail). The gels were incubated in a humid environment at 37C for 2 hours
456 to set, and then carefully removed from the chamber and placed in a digestion solution with 8
457 U/mL of Proteinase K (New England Bio, Cat # P8107S) for the designated period of time. All
458 gels in this experiment were digested on a shaker at room temperature. At the end of the
459 digestion time, the digestion solution was replaced with 1X PBS several times to wash the gels.
460 Gels were stored in 1X PBS in the dark at 4C until imaging, at which point the PBS was replaced
461 with npH2O to fully expand the gels. Gels were imaged at 10X (EC-Plan-Neofluar lens; 10x; 0.3
462 NA; 5.2mm WD) taking 10μm steps for distance on a Zeiss 710 confocal microscope with the
463 same image acquisition parameters, as described in more detail under "image acquisition".
464
465 *Digestion Time Course Analysis*
466 The ExM images from the time course experiment were analyzed with the image processing
467 program Fiji (v.+03..30, NIH). Before analysis, images were flattened across the Z dimension
468 with the *"Z Project"* function to get an idea of how many GFP positive cells were present. This
469 flattened image was only used for the selection of cells. Cells were excluded from analysis if
470 they met any of the following criteria: 1) Incomplete cell (i.e. on the image border); 2) Any cell
471 overlapping in Z with a cell already analyzed; 3) Cells with an ambiguous border or that were

472 difficult to differentiate. Given these exclusion criteria, an average of 32 cells were analyzed for
473 each time point across both animals. For some time points, cells were included from multiple
474 hippocampal sections from the same animal.
475
476 For the fluorescence analysis, each cell body meeting the inclusion criteria was manually traced
477 with the freehand selection tool in a single z section at the widest point of the cell. Once the cells
478 were traced, the *"measure"* tool in Fiji was used to measure the mean intensity and the area
479 within each individual cell ROI. To subtract background signal, one cell ROI was selected (at
480 random) and moved to a location without EGFP signal and the background mean intensity was
481 measured. The background mean intensity value was subtracted from the mean fluorescence
482 intensity of each cell from the same image, resulting in a normalized mean fluorescence. The
483 area of the cell body ROIs were used to calculate expansion factor by comparing it to the average
484 area of 37 unexpanded cell bodies, which was calculated to be 300 μm^2. To calculate the linear
485 expansion factor for each cell, we used the below formula:
486

$$\textit{Linear Expansion Factor} = \frac{\sqrt{(cell\ area)}}{\sqrt{(avg\ non\ expanded\ cell\ area)}}$$

487
488
489 A total of 159 cells were included in the analyses (average of 32 +/- 4 cells per time point from
490 two brains). The mean fluorescence and expansion factor measurements were imported into
491 Python (v 3.7, installed with the Anaconda distribution), where the average mean fluorescence
492 and average linear expansion factor were calculated for each time point, including the
493 unexpanded control (see Fig. 2). The mean fluorescence data was not normally distributed
494 (Shapiro-Wilk test for normality; $p < 0.0001$), so the mean fluorescence data was $\log_2$
495 transformed and 11 cell means were removed as outliers, pre-defined as two standard deviations
496 from the mean. These same outliers were also removed from the expansion factor data; however,
497 because this data was normally distributed (Shapiro-Wilk; $p = 0.235$), it was not transformed.
498 One-way ANOVAs were run using an ordinary least squares model with the StatsModels
499 package (ols, ANOVA_lm, statsmodels v0.11.1) comparing fluorescence intensity and linear
500 expansion factors across digestion time points. After overall significance was reached, pairwise
501 post-hoc Tukey's multiple comparison tests (pairwise_tukeyhsd, statsmodels v0.11.1) were
502 performed to determine which digestion time points were significantly different (see Fig. 2D).
503
504 *Analysis of Expanded and Unexpanded Mitochondria*
505 To determine if the ProExM protocol affects our ability to resolve and quantify mitochondria, we
506 analyzed the number and size of expanded mitochondria compared to unexpanded mitochondria.
507 Tissue from an adult male EGFP reporter mouse was immunostained with COX4 to label
508 mitochondria and expanded using our optimized ExM protocol with overnight digestion in
509 Proteinase K (see Expansion Microscopy methods). An adult male tdTomato reporter mouse was
510 similarly processed and immunostained with COX4 but not expanded. Confocal images were

511 taken of both samples for image analysis in FIJI. Note that the COX4 signal was imaged in
512 different color channels for the expanded and unexpanded samples (546nm vs 488nm,
513 respectively).
514
515 Confocal images were imported into Fiji and converted to 8-bit for the analysis. An intensity
516 threshold was chosen separately for each image which best represented the signal in the original
517 image. Using the reporter label as a guide, four cells were analyzed from the expanded sample
518 and five cells from the unexpanded sample. Cells were chosen using the same criteria as for the
519 digestion time course analysis. An ROI for each cell was drawn by fitting an oval to the cell
520 body using the oval selection tool, rotating if necessary, and the signal outside of the cell's ROI
521 was removed for the analysis. The "*nucleus counter"* plug-in from the FIJI "Cookbook"
522 microscopy analysis collection was used to segment mitochondria within the ROI of each cell
523 analyzed. The size threshold used for the expanded sample was adjusted for expansion factor,
524 which was calculated using the ratio of the cell body diameters in the expanded images
525 compared to the unexpanded images. The calculated expansion factor for the expanded images
526 was 3x in the X and Y dimensions-- an expansion factor of 9x in total area.
527
528 Once the mitochondria were properly segmented, FIJI's "*measure"* feature was used to measure
529 the number, area and intensity of each individual mitochondrial ROI. A custom Python code was
530 written to calculate and plot the averages of the mitochondria number, size and total area for the
531 expanded cells and the unexpanded cells. To account for the effect of expansion on size, the area
532 of each mitochondria was divided by the area of the soma to get a normalized mitochondria area.
533 The mitochondrial coverage was calculated by dividing the total summed mitochondrial area in
534 the cell by the area of the cytoplasm (*soma area – nucleus area*) and converting it to a
535 percentage.
536
537 **Image acquisition**
538 Images were acquired on an upright Zeiss 710 confocal microscope equipped with a motorized
539 stage, 488/561/633 laser lines, and 20X/1.0 NA water immersion or 20X/0.4 NA air lenses. Gels
540 were expanded by washing with 0.001X PBS three times and by incubating overnight at RT in
541 0.001X PBS. Gels were immobilized in 50mm glass bottom wells (WillCo Wells, HBSB-5040)
542 by applying 2% agarose to the edges of the gels. Gels were then imaged in a fully expanded state
543 in or 0.001X PBS.
544
545 **ExM image processing**
546 Czi files were imported into Fiji, individual channel images were split and adjusted for
547 brightness and contrast equivalently across conditions, then images were viewed with the volume
548 viewer plugin (v. 2.01.2). If images showed considerable shift or too many neurons overlapped, a
549 subset stack was created without the offending Z sections. Mode was set to max-projection and
550 interpolation was set to tricubic smooth with z-aspect and sampling optimized per image

(typically 0.5-2.0 for each parameter). Snapshots were taken in the XY plane at 1.0 and 2.0 scale in grayscale and 1D. The resulting snapshot images were imported into Photoshop (v. 21.2) and converted to 300 dpi. Any further brightness and contrast edits done in photoshop were minimal and applied equivalently to all comparable images in the figure.

Statistical analyses

Statistical analyses were done in python (v 3.7) with an alpha of 0.05 considered significant.

Acknowledgements

Research reported in this publication was supported by the National Institute of Mental Health of the NIH under award R00MH109626 to S.F. We thank the members of the Dudek lab for feedback and critically reading this manuscript, as well as the Virginia Tech animal care staff for their support.

Author Contributions

Conceptualization, S.F.; Methodology, L.A.C., K.E.P., N.A.S., D.L., S.F.; Formal Analysis, L.A.C., K.E.P., N.A.S., S.F.; Investigation, L.A.C., K.E.P., N.A.S., D.L., S.F.; Writing – Original Draft, L.A.C., K.E.P., S.F.; Writing – Review & Editing, L.A.C., K.E.P., S.F.; Visualization, L.A.C., K.E.P., S.F.; Supervision, S.F.; Funding Acquisition, S.F.

Declaration of Interests

The authors declare no conflict of interest or competing financial interest.

575 **FIGURE LEGENDS**
576
577 **Fig. 1: ExM workflow for visualizing subcellular organelles in fixed brain tissue.**
578 Schematic of immunostaining and proExM workflows tested to optimize visualization of
579 organelles in genetically-labeled neurons.
580
581 **Fig. 2: The effect of Proteinase K digestion time on fluorescence intensity and expansion**
582 **factor.**
583 **A)** Representative single z-section images of unexpanded (i) and expanded GFP+ CA2 neurons
584 after 2-hour (ii), 4-hour (iii), 8-hour (iv), or overnight (v) digestion with Proteinase K. Image
585 acquisition parameters were identical for each condition, except for the unexpanded condition.
586 **B)** GFP fluorescence intensity measured in the cell soma after the different digestion times.
587 Fluorescence was corrected for background and $\log_2$ transformed. Line represents the median.
588 Digestion time had a significant effect on GFP fluorescence (one-way ANOVA; F-stat: 20.96, p-
589 value: 8.17E-14, 32 ± 4 cells per time point from two animals, 159 total cells).
590 **C)** Expansion factor of the expanded cell somas in **B**. Expansion factors were calculated using
591 cell soma areas relative to the average unexpanded cell soma area. Line represents the median.
592 Digestion time had a significant effect on expansion factor (one-way ANOVA; F-stat: 21.07, p-
593 value: 4.26E-11).
594 **D)** Matrix of p-values visualizing the results of pairwise Tukey's post hoc tests comparing mean
595 fluorescence (upper diagonal) or expansion factor (lower diagonal) at each digestion time point.
596 Matrix is color coded by p-value (red = significant; grey = not significant; α=0.05).
597 **E)** Effect of digestion time on fluorescence intensity (cyan; left axis) and expansion factor
598 (orange; right axis). Plot shows the mean and 95% confidence intervals from **B** and **C**.
599 **F)** Unexpanded (i) and overnight expanded (ii) max-projection 10X confocal images of GFP+
600 CA2 cells. Images are the same as in **A**(i) and (v). Imaging parameters were optimized separately
601 to obtain the best image of both.
602 Scale bars = (**A**, **F**) 50 μm.
603
604 **Fig. 3: No appreciable effect of tissue depth on expansion factor.**
605 **A)** Average cell soma area (in μm^2) by Z section depth for unexpanded control and digestion
606 conditions. Cell soma area was measured in the Z section with the widest soma diameter.
607 Because of the overall increase in depth with expansion, cells were binned by Z section to
608 achieve ~6 bins per time point. N = 32 ± 4 cells per time point.
609 **B)** Background subtracted average cell soma fluorescence by Z section depth. Binning of the
610 data is the same as in A. The data are not $\log_2$ transformed as in Fig. 2.
611 **C)** Representative confocal images of GFP+ CA2 cell somas after 2-hour (left panel) or
612 overnight (right panel) digestion at three Z-section depths. Cell soma size and fluorescence is
613 variable in the Z dimension in unexpanded conditions, which does not appreciably change under
614 difference digestion conditions.

615 Error bars show the standard deviation. Scale bar is 50µm.
616
617 **Fig. 4: ProExM pipeline comparison for visualizing mitochondria.**
618 **A)** 20X Max-projection image of a section immunostained for COX4 (i) and RFP (iii) pre-ExM
619 with autoclave digestion. Images in panels A-D were acquired with identical imaging parameters
620 to directly compare conditions. Brightness and contrast were adjusted to the same extent across
621 the entire image.
622 **B)** 20X Max-projection image of a boiled section immunostained for COX4 (i) and RFP (ii) pre-
623 ExM with overnight Proteinase K digestion.
624 **C)** 20X Max-projection image of a section immunostained for COX4 (i) and RFP (ii) post-ExM
625 with autoclave digestion.
626 **D)** 20X Max-projection image of a boiled section immunostained for COX4 (i) and RFP (ii)
627 post-ExM with overnight Proteinase K digestion
628 **E)** 40X Max-projection image from a subset of Z sections from a boiled, unexpanded section
629 immunostained for COX4 and RFP. Inset is a single Z section from the indicated representative
630 cell (white asterisk) with mitochondria outlined as quantified in G-I. Imaging parameters were
631 optimized per condition in E-F.
632 **F)** 20X Max-projection image from a subset of Z sections from a boiled section immunostained
633 for COX4 and GFP pre-ExM with overnight Proteinase K digestion as in **B.**
634 **G)** The average number of mitochondria per cell in unexpanded **(E)** and expanded **(F)** sections.
635 **H)** Mitochondria area per cell (normalized by soma area). Line reflects median and whiskers are
636 twice the inner quartile range.
637 **I)** The average percent cytoplasm area (soma area - nuclear area) containing mitochondria. Note
638 that ExM better resolves densely packed mitochondria, resulting in greater number, smaller
639 sized, and fewer percent area per cell soma compared with no-ExM.
640 Scale bars: 50 µm (**A,E,F**) and 5 µm (insets).
641
642 **Fig. 5: ProExM pipeline comparison for visualizing Golgi.**
643 **A)** 20X Max-projection image of a section immunostained for GOLGA5 (i) and GFP (iii) pre-
644 ExM with autoclave digestion. (ii) Insets are zoomed images of the dotted box in (i). Images in
645 panels **A-C** were acquired with identical imaging parameters to directly compare conditions.
646 Brightness and contrast were adjusted to the same extent across the entire image.
647 **B)** 20X Max-projection image of a section immunostained for GOLGA5 (i) and GFP (iii) pre-
648 ExM with overnight Proteinase K digestion.
649 **C)** 20X Max-projection image of a section immunostained for GOLGA5 (i) and GFP (iii) post-
650 ExM with overnight Proteinase K digestion.
651 **D)** 40X Max-projection of a subset of Z sections from an unexpanded section immunostained for
652 GOLGA5 (i) and RFP (iii). Imaging parameters were optimized per condition in **D-E**.
653 **E)** 20X Max-projection of a subset of Z sections from image in (**B**) immunostained pre-ExM
654 with overnight Proteinase K digestion. Note the increase in Golgi complexity that is resolved

655 with autoclave or Proteinase K digested gels compared with unexpanded sections, although
656 fluorescence intensity was better retained with Proteinase K digestion.
657 **F)** Line plot profile showing the fluorescence intensity of unexpanded Golgi (cyan) and Golgi
658 after IHC-pre-ExM with Proteinase K digestion (magenta). Measured Golgi are inset in **Diii** and
659 **E.**
660 Scale bars: 50µm (**Ai, Di, E**) and 10µm (**Aii, Dii**).
661
662 **Fig. 6: Resolving dendritic spines with ExM.**
663 **A**) 20X with 3X zoom max-projection image (i) of a section immunostained for RFP pre-ExM
664 with overnight Proteinase K digestion. This mouse received 2 tamoxifen injections. (ii) Insets are
665 2X zoomed images of the dotted box in (i). Images were acquired with imaging parameters
666 optimal per condition. Brightness and contrast were adjusted per condition across the entire
667 image.
668 **B**) 40X with 2X zoom max-projection image of an unexpanded tdTomato section. This mouse
669 received 2 tamoxifen injections.
670 **C**) 20X with 2X zoom max-projection image of a section immunostained for GFP pre-ExM with
671 overnight Proteinase K digestion.
672 **D**) 40X with 2X zoom max-projection image from an unexpanded section immunostained for
673 GFP. Note the increased background labeling and density of dendritic branches in the
674 unexpanded images, making dendrites more difficult to trace compared with expanded images.
675 Scale bars: 25µm (Ai, Bi, Ci, Di) and 5µm (Aii, Bii, Cii, Dii).
676

677 **REFERENCES**

678 1. Chozinski TJ, Halpern AR, Okawa H, Kim H-J, Tremel GJ, Wong ROL, Vaughan JC.
679 Expansion microscopy with conventional antibodies and fluorescent proteins. Nature
680 Methods. Nature Publishing Group; 2016 Jun;13(6):485–488.

681 2. Tillberg PW, Chen F, Piatkevich KD, Zhao Y, Yu C-CJ, English BP, Gao L, Martorell A,
682 Suk H-J, Yoshida F, DeGennaro EM, Roossien DH, Gong G, Seneviratne U, Tannenbaum
683 SR, Desimone R, Cai D, Boyden ES. Protein-retention expansion microscopy of cells and
684 tissues labeled using standard fluorescent proteins and antibodies. Nat Biotechnol.
685 2016;34(9):987–992. PMCID: PMC5068827

686 3. Asano SM, Gao R, Wassie AT, Tillberg PW, Chen F, Boyden ES. Expansion Microscopy:
687 Protocols for Imaging Proteins and RNA in Cells and Tissues. Curr Protoc Cell Biol.
688 2018;80(1):e56. PMCID: PMC6158110

689 4. Ku T, Swaney J, Park J-Y, Albanese A, Murray E, Cho JH, Park Y-G, Mangena V, Chen J,
690 Chung K. Multiplexed and scalable super-resolution imaging of three-dimensional protein
691 localization in size-adjustable tissues. Nat Biotechnol. 2016;34(9):973–981. PMCID:
692 PMC5070610

693 5. Park H-E, Choi D, Park JS, Sim C, Park S, Kang S, Yim H, Lee M, Kim J, Pac J, Rhee K,
694 Lee J, Lee Y, Lee Y, Kim S-Y. Scalable and Isotropic Expansion of Tissues with Simply
695 Tunable Expansion Ratio. Adv Sci (Weinh). 2019 Nov;6(22):1901673. PMCID:
696 PMC6864509

697 6. Gambarotto D, Zwettler FU, Le Guennec M, Schmidt-Cernohorska M, Fortun D, Borgers S,
698 Heine J, Schloetel J-G, Reuss M, Unser M, Boyden ES, Sauer M, Hamel V, Guichard P.
699 Imaging cellular ultrastructures using expansion microscopy (U-ExM). Nat Methods.
700 2019;16(1):71–74. PMCID: PMC6314451

701 7. Katoh Y, Chiba S, Nakayama K. Practical method for superresolution imaging of primary
702 cilia and centrioles by expansion microscopy using an amplibody for fluorescence signal
703 amplification. Mol Biol Cell. 2020 15;31(20):2195–2206. PMCID: PMC7550703

704 8. Shi X, Li Q, Dai Z, Tran AA, Feng S, Ramirez AD, Lin Z, Wang X, Chow TT, Seiple IB,
705 Huang B. Label-retention expansion microscopy. bioRxiv. Cold Spring Harbor Laboratory;
706 2019 Jul 2;687954.

707 9. Truckenbrodt S, Sommer C, Rizzoli SO, Danzl JG. A practical guide to optimization in X10
708 expansion microscopy. Nature Protocols. Nature Publishing Group; 2019 Mar;14(3):832–
709 863.

710 10. Chen F, Tillberg PW, Boyden ES. Expansion microscopy. Science. 2015 Jan
711 30;347(6221):543–548. PMID: 25592419

712 11. Wassie AT, Zhao Y, Boyden ES. Expansion microscopy: principles and uses in biological
713 research. Nat Methods. 2019;16(1):33–41. PMCID: PMC6373868

714 12. Kunz TC, Götz R, Gao S, Sauer M, Kozjak-Pavlovic V. Using Expansion Microscopy to
715 Visualize and Characterize the Morphology of Mitochondrial Cristae. Front Cell Dev Biol.
716 2020;8:617. PMCID: PMC7373753

717 13. Büttner M, Lagerholm CB, Waithe D, Galiani S, Schliebs W, Erdmann R, Eggeling C,
718 Reglinski K. Challenges of Using Expansion Microscopy for Super-resolved Imaging of
719 Cellular Organelles. Chembiochem. 2020 Oct 13; PMID: 33049107

720 14. Pesce L, Cozzolino M, Lanzanò L, Diaspro A, Bianchini P. Measuring expansion from
721 macro- to nanoscale using NPC as intrinsic reporter. J Biophotonics.
722 2019;12(8):e201900018. PMCID: PMC7065622

723 15. Sun D, Fan X, Zhang H, Huang Z, Tang Q, Li W, Bai J, Lei X, Chen X. Click-ExM enables
724 expansion microscopy for all biomolecules. bioRxiv. Cold Spring Harbor Laboratory; 2020
725 Mar 20;2020.03.19.998039.

726 16. Pernal SP, Liyanaarachchi A, Gatti DL, Formosa B, Pulvender R, Kuhn ER, Ramos R, Naik
727 AR, George K, Arslanturk S, Taatjes DJ, Jena BP. Nanoscale imaging using differential
728 expansion microscopy. Histochem Cell Biol. 2020 Jun;153(6):469–480. PMID: 32193594

729 17. Zhao Y, Bucur O, Irshad H, Chen F, Weins A, Stancu AL, Oh E-Y, DiStasio M, Torous V,
730 Glass B, Stillman IE, Schnitt SJ, Beck AH, Boyden ES. Nanoscale imaging of clinical
731 specimens using pathology-optimized expansion microscopy. Nat Biotechnol. 2017
732 Aug;35(8):757–764. PMCID: PMC5548617

733 18. Götz R, Panzer S, Trinks N, Eilts J, Wagener J, Turrà D, Di Pietro A, Sauer M, Terpitz U.
734 Expansion Microscopy for Cell Biology Analysis in Fungi. Front Microbiol. 2020;11:574.
735 PMCID: PMC7147297

736 19. Düring DN, Rocha MD, Dittrich F, Gahr M, Hahnloser RHR. Expansion Light Sheet
737 Microscopy Resolves Subcellular Structures in Large Portions of the Songbird Brain. Front
738 Neuroanat. 2019;13:2. PMCID: PMC6365838

739 20. Jiang N, Kim H-J, Chozinski TJ, Azpurua JE, Eaton BA, Vaughan JC, Parrish JZ.
740 Superresolution imaging of Drosophila tissues using expansion microscopy. Mol Biol Cell.
741 2018 15;29(12):1413–1421. PMCID: PMC6014096

742 21. Cahoon CK, Yu Z, Wang Y, Guo F, Unruh JR, Slaughter BD, Hawley RS. Superresolution
743 expansion microscopy reveals the three-dimensional organization of the Drosophila
744 synaptonemal complex. Proc Natl Acad Sci U S A. 2017 15;114(33):E6857–E6866. PMCID:
745 PMC5565445

746 22. Gao R, Asano SM, Upadhyayula S, Pisarev I, Milkie DE, Liu T-L, Singh V, Graves A,
747 Huynh GH, Zhao Y, Bogovic J, Colonell J, Ott CM, Zugates C, Tappan S, Rodriguez A,
748 Mosaliganti KR, Sheu S-H, Pasolli HA, Pang S, Xu CS, Megason SG, Hess H, Lippincott-
749 Schwartz J, Hantman A, Rubin GM, Kirchhausen T, Saalfeld S, Aso Y, Boyden ES, Betzig
750 E. Cortical column and whole-brain imaging with molecular contrast and nanoscale
751 resolution. Science. 2019 Jan 18;363(6424).

752 23. Fecher C, Trovò L, Müller SA, Snaidero N, Wettmarshausen J, Heink S, Ortiz O, Wagner I,
753 Kühn R, Hartmann J, Karl RM, Konnerth A, Korn T, Wurst W, Merkler D, Lichtenthaler SF,
754 Perocchi F, Misgeld T. Cell-type-specific profiling of brain mitochondria reveals functional
755 and molecular diversity. Nature Neuroscience. 2019 Oct;22(10):1731–1742.

756 24. Karagiannis ED, Kang JS, Shin TW, Emenari A, Asano S, Lin L, Costa EK, Consortium
757 IGC, Marblestone AH, Kasthuri N, Boyden ES. Expansion Microscopy of Lipid Membranes.
758 bioRxiv. Cold Spring Harbor Laboratory; 2019 Nov 4;829903.

759 25. Martínez GF, Gazal NG, Quassollo G, Szalai AM, Cid-Pellitero ED, Durcan TM, Fon EA,
760 Bisbal M, Stefani FD, Unsain N. Quantitative expansion microscopy for the characterization
761 of the spectrin periodic skeleton of axons using fluorescence microscopy. Sci Rep. 2020
762 19;10(1):2917. PMCID: PMC7031372

763 26. Scheible MB, Tinnefeld P. Quantifying Expansion Microscopy with DNA Origami
764 Expansion Nanorulers. bioRxiv. Cold Spring Harbor Laboratory; 2018 Feb 14;265405.

765 27. Vanheusden M, Vitale R, Camacho R, Janssen KPF, Acke A, Rocha S, Hofkens J.
766 Fluorescence Photobleaching as an Intrinsic Tool to Quantify the 3D Expansion Factor of
767 Biological Samples in Expansion Microscopy. ACS Omega. 2020 Mar 17;5(12):6792–6799.
768 PMCID: PMC7114699

769 28. Min K, Cho I, Choi M, Chang J-B. Multiplexed expansion microscopy of the brain through
770 fluorophore screening. Methods. 2020 01;174:3–10. PMID: 31326595

771 29. Steward O, Schuman EM. Protein synthesis at synaptic sites on dendrites. Annu Rev
772 Neurosci. 2001;24:299–325. PMID: 11283313

773 30. Pierce JP, Mayer T, McCarthy JB. Evidence for a satellite secretory pathway in neuronal
774 dendritic spines. Curr Biol. 2001 Mar 6;11(5):351–355. PMID: 11267872

775 31. Bowen AB, Bourke AM, Hiester BG, Hanus C, Kennedy MJ. Golgi-independent secretory
776 trafficking through recycling endosomes in neuronal dendrites and spines. Elife. 2017 06;6.
777 PMCID: PMC5624785

778 32. Kennedy MJ, Ehlers MD. ORGANELLES AND TRAFFICKING MACHINERY FOR
779 POSTSYNAPTIC PLASTICITY. Annual Review of Neuroscience. 2006 Jul 21;29(1):325–
780 362.

781 33. Alexander GM, Brown LY, Farris S, Lustberg D, Pantazis C, Gloss B, Plummer NW, Jensen
782 P, Dudek SM. CA2 neuronal activity controls hippocampal low gamma and ripple
783 oscillations. Elife. 2018 02;7. PMCID: PMC6251629

784 34. Schindelin J, Arganda-Carreras I, Frise E, Kaynig V, Longair M, Pietzsch T, Preibisch S,
785 Rueden C, Saalfeld S, Schmid B, Tinevez J-Y, White DJ, Hartenstein V, Eliceiri K,
786 Tomancak P, Cardona A. Fiji: an open-source platform for biological-image analysis. Nat
787 Methods. 2012 Jun 28;9(7):676–682. PMCID: PMC3855844

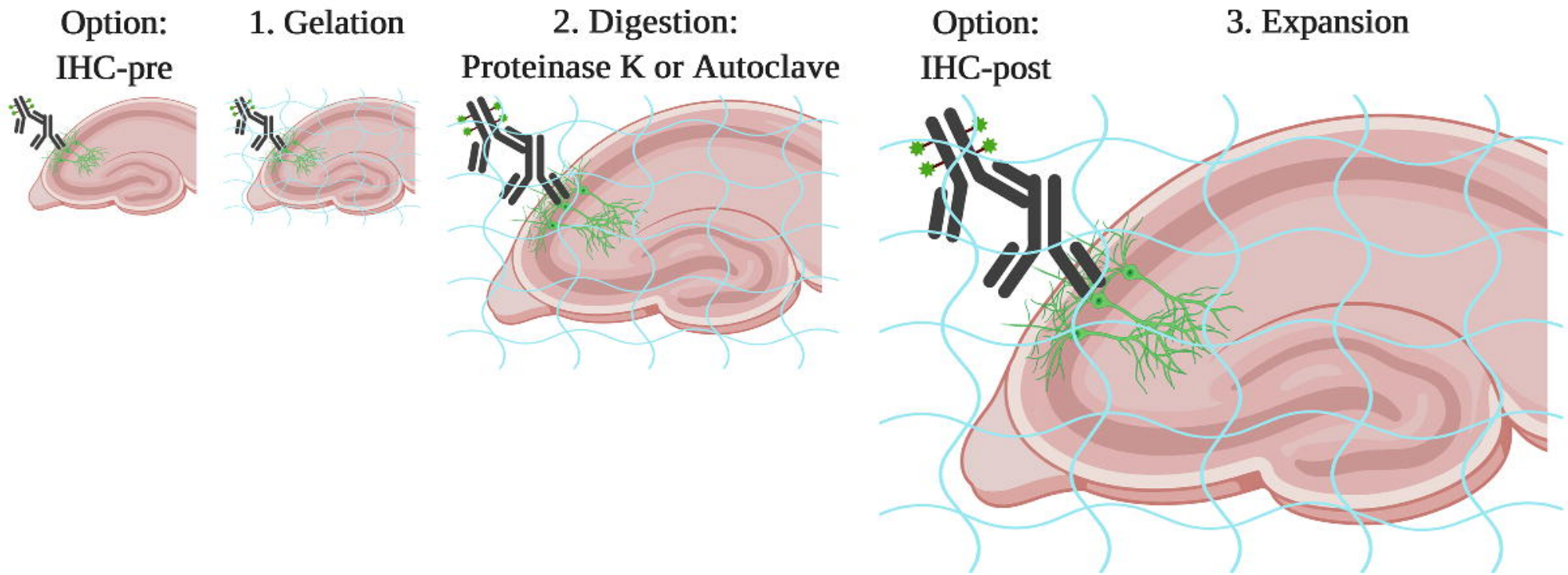

Figure 1: ExM workflow for visualizing subcellular organelles in fixed brain tissue.
Schematic of immunostaining and proExM workflows tested to optimize visualization of organelles in genetically-labeled neurons.

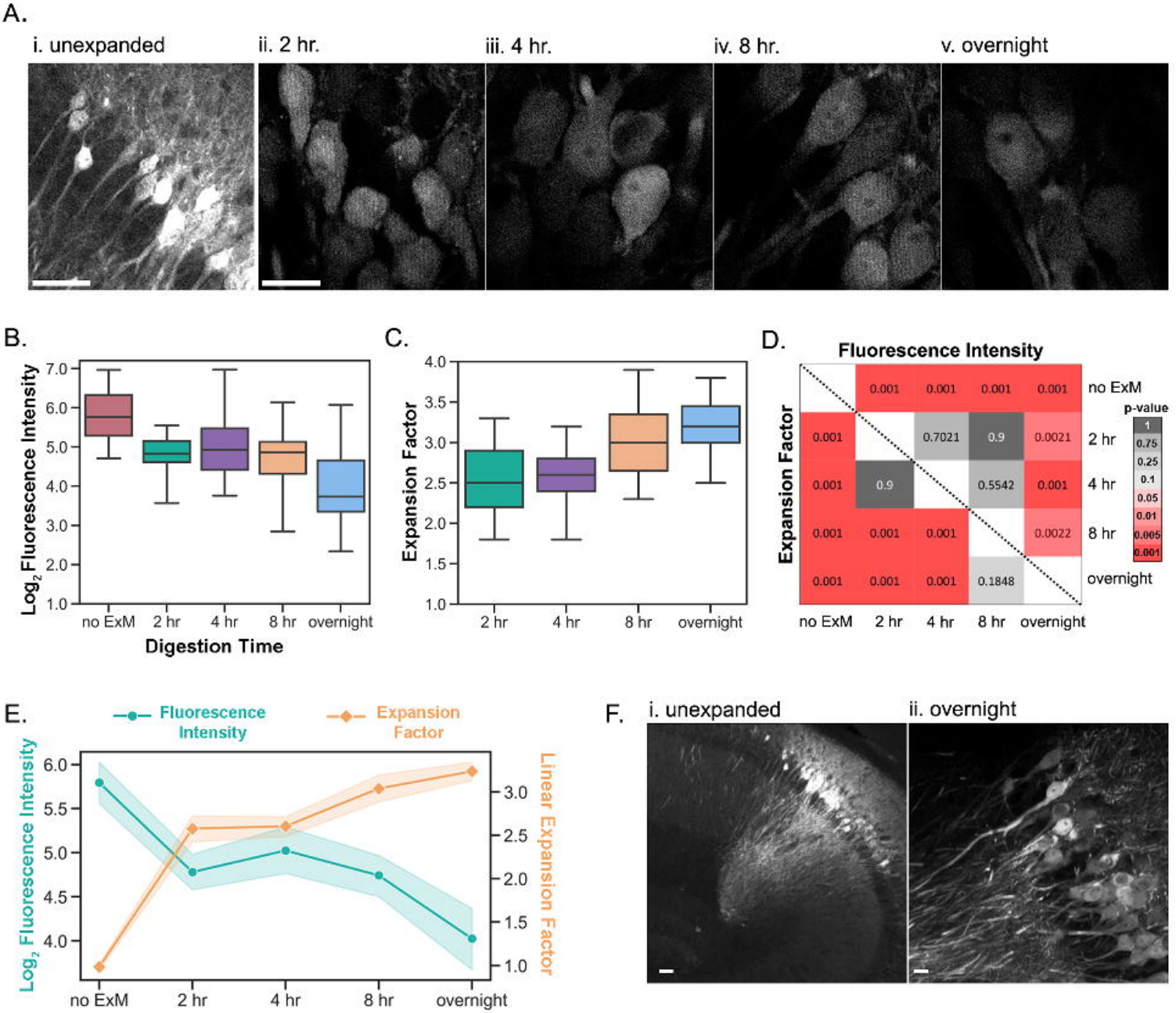

Figure 2: The effect of Proteinase K digestion time on fluorescence intensity and expansion factor.
A) Representative single z-section images of unexpanded (i) and expanded GFP+ CA2 neurons after 2-hour (ii), 4-hour (iii), 8-hour (iv), or overnight (v) digestion with Proteinase K. Image acquisition parameters were identical for each condition, except for the unexpanded condition.
B) GFP fluorescence intensity measured in the cell soma after the different digestion times. Fluorescence was corrected for background and $\log_2$ transformed. Line represents the median. Digestion time had a significant effect on GFP fluorescence (one-way ANOVA; F-stat: 20.96, p-value: 8.17E-14, 32 ± 4 cells per time point from two animals, 159 total cells).
C) Expansion factor of the expanded cell somas in B. Expansion factors were calculated using cell soma areas relative to the average unexpanded cell soma area. Digestion time had a significant effect on expansion factor (one-way ANOVA; F-stat: 21.07, p-value: 4.26E-11).
D) Matrix of p-values visualizing the results of pairwise Tukey's post hoc tests comparing mean fluorescence (upper diagonal) or expansion factor (lower diagonal) at each digestion time point. Matrix is color coded by p-value (red = significant; grey = not significant; α=0.05).
E) Effect of digestion time on fluorescence intensity (cyan; left axis) and expansion factor (orange; right axis). Plot shows the mean and 95% confidence intervals from **B** and **C**.
F) Unexpanded (i) and overnight expanded (ii) max-projection 10X confocal images of GFP+ CA2 cells. Images are the same as in **A**(i) and (v). Imaging parameters were optimized separately to obtain the best image of both. Scale bars = (**A**, **F**) 50 µm.

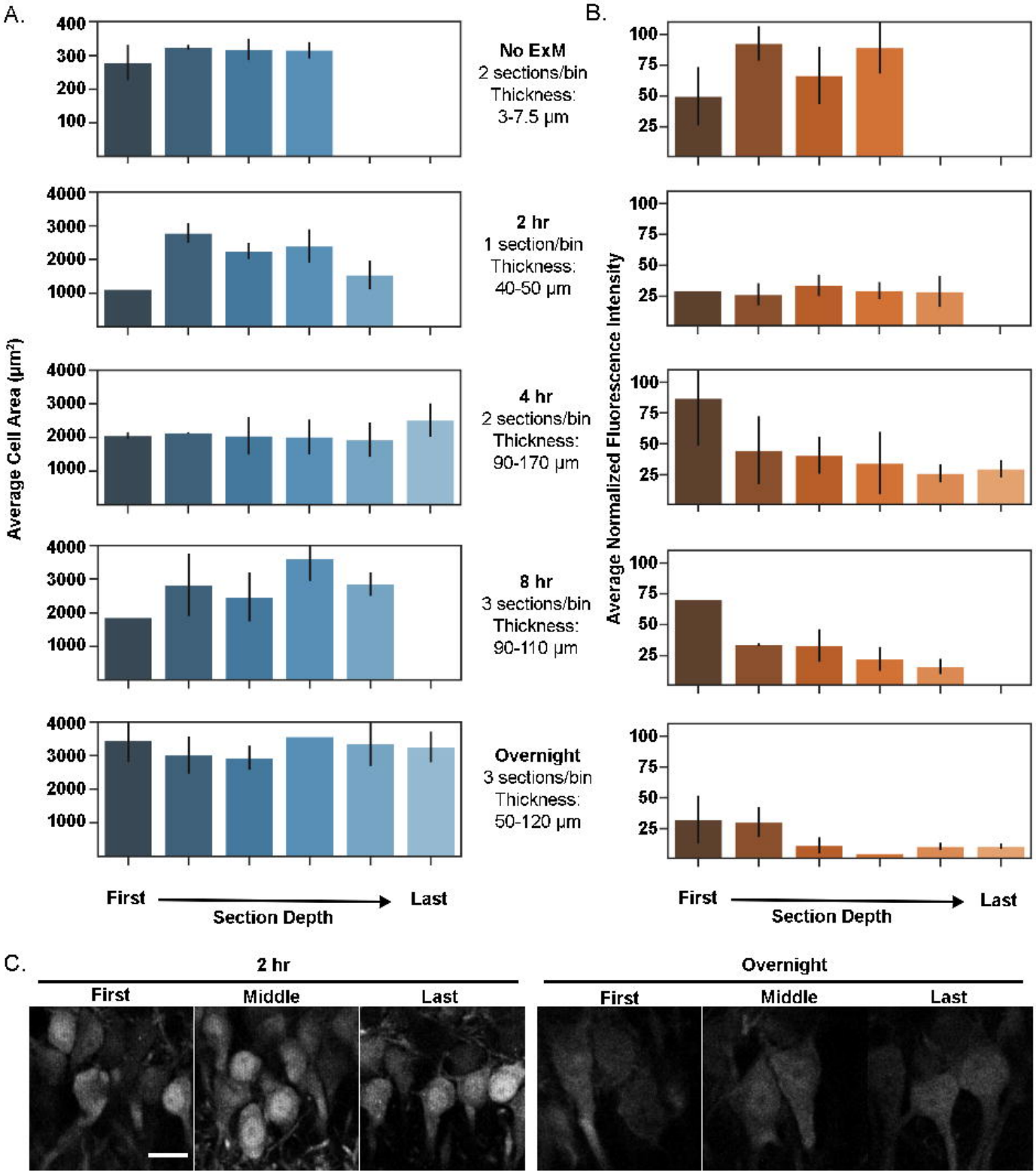

Figure 3: No appreciable effect of tissue depth on expansion factor.
A) Average cell soma area (in µm²) by Z section depth for unexpanded control and digestion conditions. Cell soma area was measured in the Z section with the widest soma diameter. Because of the overall increase in depth with expansion, cells were binned by Z section to achieve ~6 bins per time point. N = 32 ± 4 cells per time point.
B) Background subtracted average cell soma fluorescence by Z section depth. Binning of the data is the same as in A. The data are not $\log_2$ transformed as in Fig 2.
C) Representative confocal images of GFP+ CA2 cell somas after 2-hour (left panel) or overnight (right panel) digestion at three Z-section depths. Cell soma size and fluorescence is variable in the Z dimension in unexpanded conditions, which does not appreciably change under difference digestion conditions. Error bars show the standard deviation. Scale bar is 50µm.

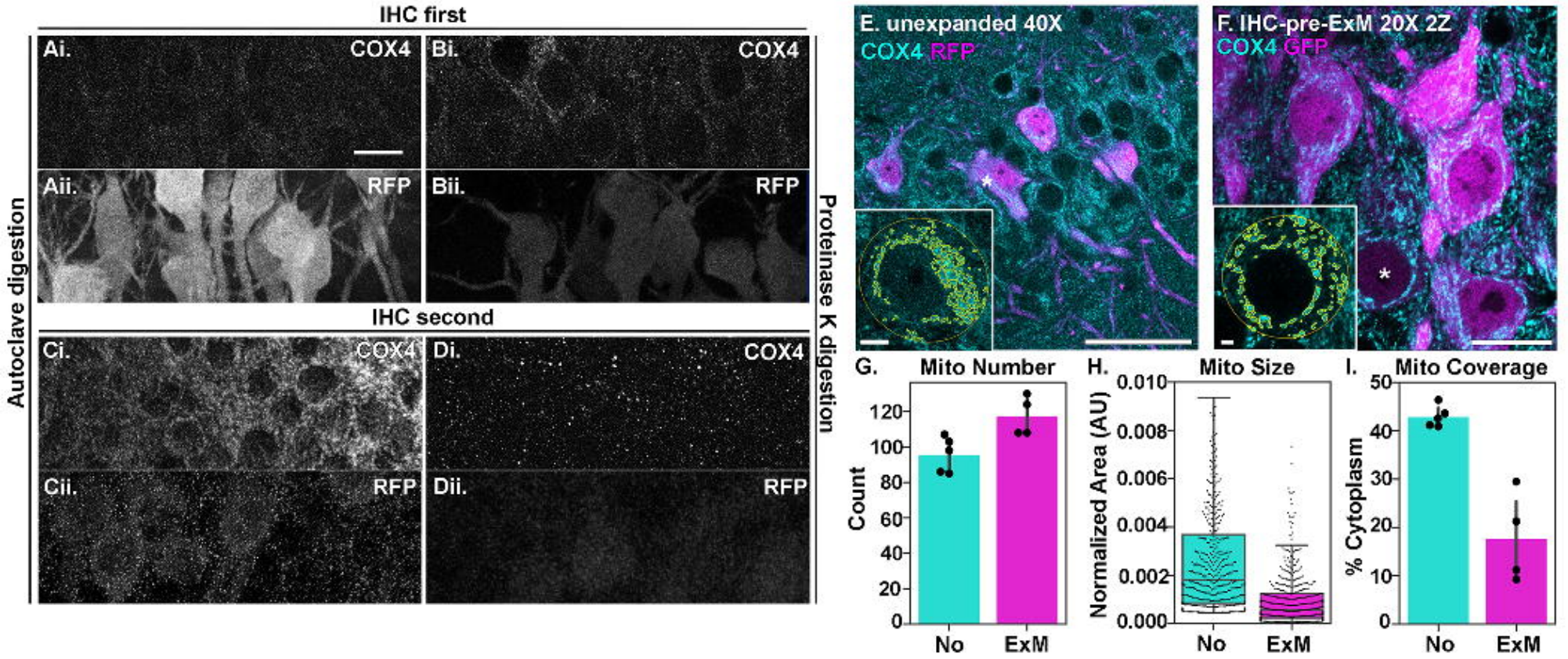

Figure 4: ProExM pipeline comparison for visualizing mitochondria.

A) 20X Max-projection image of a section immunostained for COX4 (i) and RFP (ii) pre-ExM with autoclave digestion. Images in panels A-D were acquired with identical imaging parameters to directly compare conditions. Brightness and contrast were adjusted to the same extent across the entire image.

B) 20X Max-projection image of a boiled section immunostained for COX4 (i) and RFP (ii) pre-ExM with overnight Proteinase K digestion.

C) 20X Max-projection image of a section immunostained for COX4 (i) and RFP (ii) post-ExM with autoclave digestion.

D) 20X Max-projection image of a boiled section immunostained for COX4 (i) and RFP (ii) post-ExM with overnight Proteinase K digestion

E) 40X Max-projection image from a subset of Z sections from a boiled, unexpanded section immunostained for COX4 and RFP. Inset is a single Z section from the indicated representative cell (white asterisk) with mitochondria outlined as quantified in **G-I**. Imaging parameters were optimized per condition in **E-F**.

F) 20X Max-projection image from a subset of Z sections from a boiled section immunostained for COX4 and GFP pre-ExM with overnight Proteinase K digestion as in **B**.

G) The average number of mitochondria per cell in unexpanded **(E)** and expanded **(F)** sections.

H) Mitochondria area per cell (normalized by soma area). Line reflects median and whiskers are twice the inner quartile range.

I) The average percent cytoplasm area (soma area - nuclear area) containing mitochondria. Note that ExM better resolves densely packed mitochondria, resulting in greater number, smaller sized, and fewer percent area per cell soma compared with non-ExM.

Scale bars: 50 µm (**A**,**E**,**F**) and 5 µm (insets).

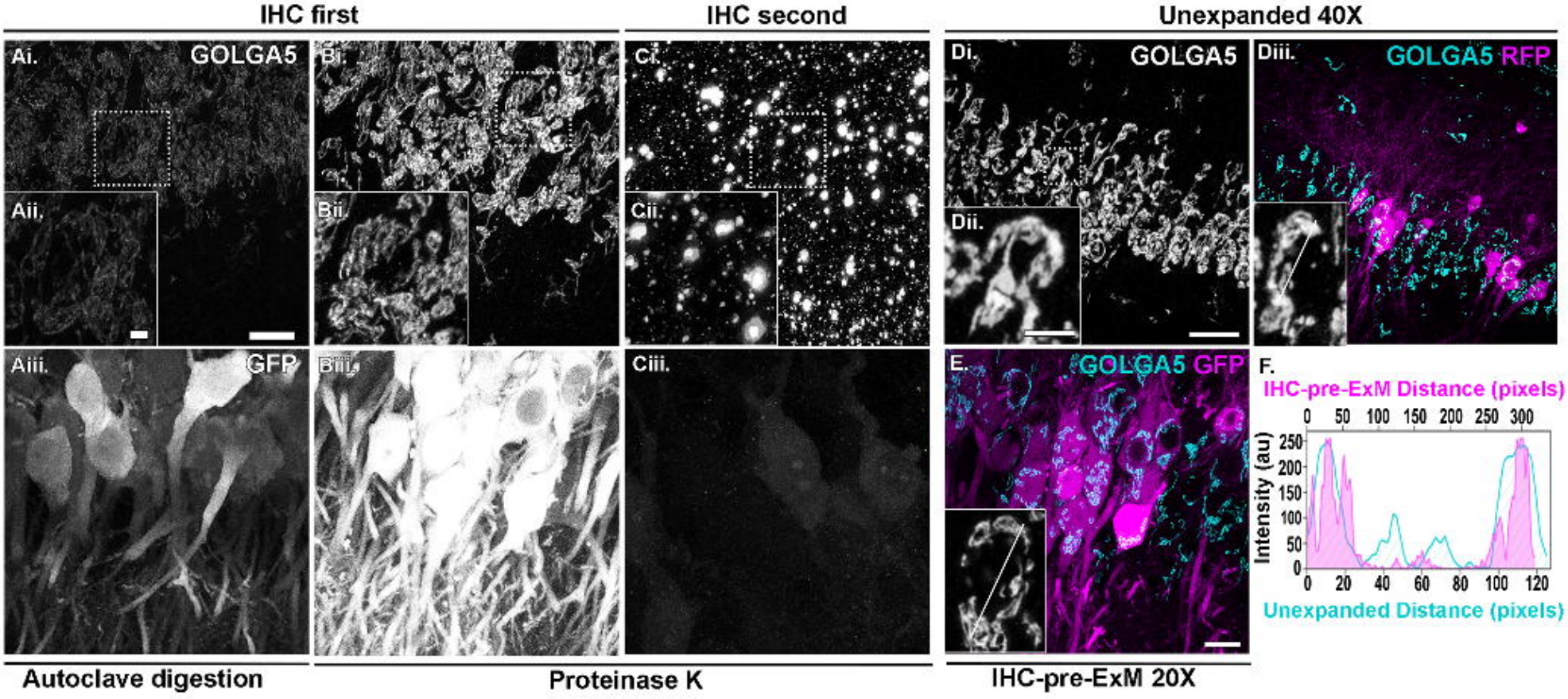

Figure 5: ProExM pipeline comparison for visualizing Golgi.

A) 20X Max-projection image of a section immunostained for GOLGA5 (i) and GFP (iii) pre-ExM with autoclave digestion. (ii) Insets are zoomed images of the dotted box in (i). Images in panels **A-C** were acquired with identical imaging parameters to directly compare conditions. Brightness and contrast were adjusted to the same extent across the entire image.

B) 20X Max-projection image of a section immunostained for GOLGA5 (i) and GFP (iii) pre-ExM with overnight Proteinase K digestion.

C) 20X Max-projection image of a section immunostained for GOLGA5 (i) and GFP (iii) post-ExM with overnight Proteinase K digestion.

D) 40X Max-projection of a subset of Z sections from an unexpanded section immunostained for GOLGA5 (i) and RFP (iii). Imaging parameters were optimized per condition in **D-E**.

E) 20X Max-projection of a subset of Z sections from image in (**B**) immunostained pre-ExM with overnight Proteinase K digestion. Note the increase in Golgi complexity that is resolved with autoclave or Proteinase K digested gels compared with unexpanded sections, although fluorescence intensity was better retained with Proteinase K digestion.

F) Line plot profile showing the fluorescence intensity of unexpanded Golgi (cyan) and Golgi after IHC-pre-ExM with Proteinase K digestion (magenta). Measured Golgi are insets in **Diii** and **E**.

Scale bars: 50μm (**A**i, **D**i, **E**) and 10μm (**A**ii, **D**ii).

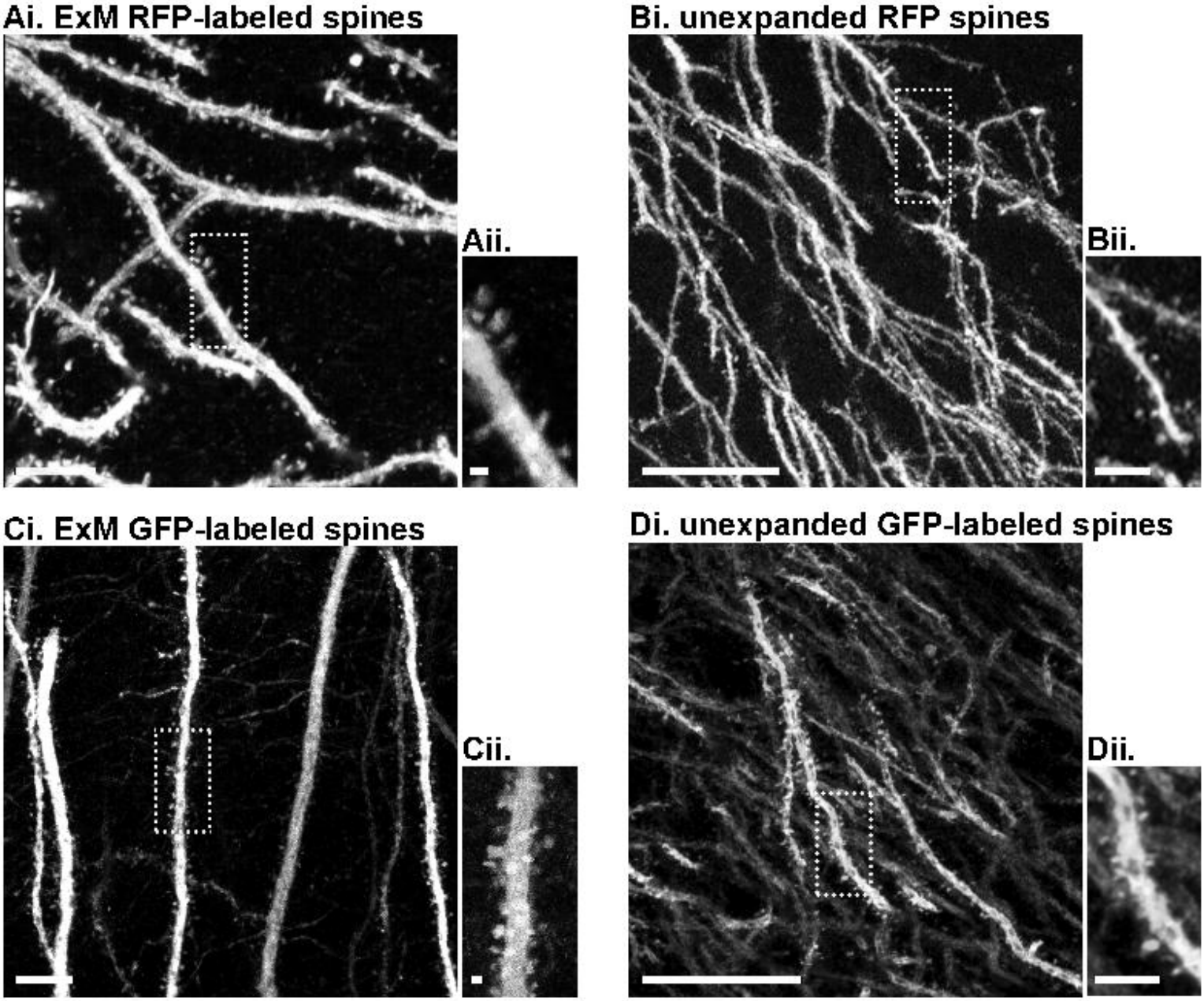

Figure 6: Resolving dendritic spines with ExM.
A) 20X with 3X zoom max-projection image (i) of a section immunostained for RFP pre-ExM with overnight Proteinase K digestion. This mouse received 2 tamoxifen injections. (ii) Insets are 2X zoomed images of the dotted box in (i). All images were acquired with parameters optimal per condition. Brightness and contrast were adjusted per condition across the entire image.
B) 40X with 2X zoom max-projection image of an unexpanded tdTomato section. This mouse received 2 tamoxifen injections.
C) 20X with 2X zoom max-projection image of a section immunostained for GFP pre-ExM with overnight Proteinase K digestion.
D) 40X with 2X zoom max-projection image from an unexpanded section immunostained for GFP. Note the increased background labeling and density of dendritic branches in the unexpanded images, making dendrites more difficult to trace compared with expanded images.
Scale bars: 25μm (**Ai**, **Bi**, **Ci**, **Di**) and 5μm (**Aii**, **Bii**, **Cii**, **Dii**).